The University of Manchester Institute of Science and Technology
PO Box 88, Manchester M60 1QD. Telephone 061-236 3311. Telex 666094

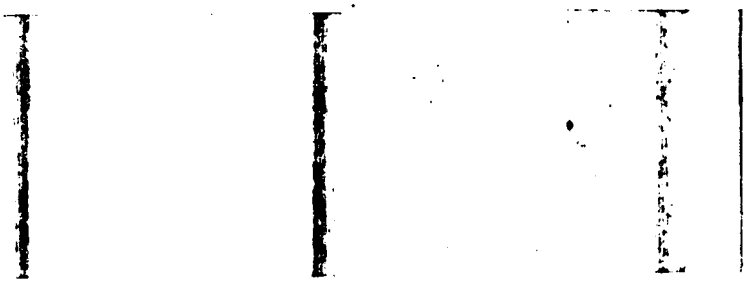

DISCLAIMER NOTICE

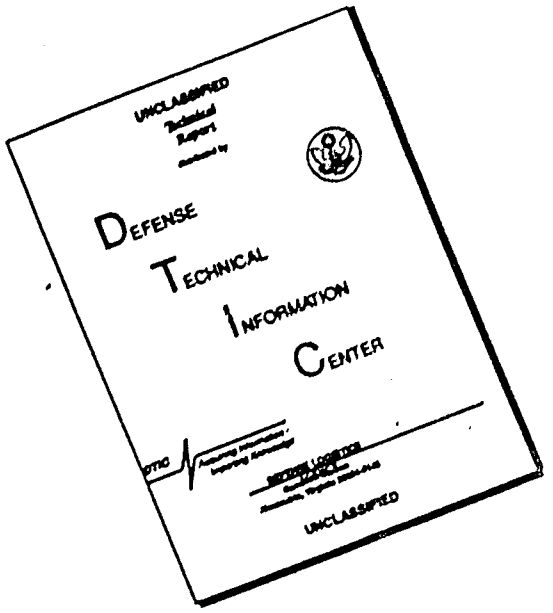

THIS DOCUMENT IS BEST QUALITY AVAILABLE. THE COPY FURNISHED TO DTIC CONTAINED A SIGNIFICANT NUMBER OF PAGES WHICH DO NOT REPRODUCE LEGIBLY.

A LABORATORY STUDY OF AIRCRAFT PRECIPITATION STATIC CHARGING

Contract N° AFOSR-82-0323

Dr. A.J. Illingworth
Physics Department
UMIST
Manchester M60 1QD
England

May 1984

Final Scientific Report 1982 - 1983

Approved for public release: distribution unlimited

Prepared for
Wright Aeronautical Laboratories
and
EUROPEAN OFFICE OF AEROSPACE RESEARCH AND DEVELOPMENT
London, England

UNCLASSIFIED

SECURITY CLASSIFICATION OF THIS PAGE (When Data Entered)

REPORT DOCUMENTATION PAGE

READ INSTRUCTIONS BEFORE COMPLETING FORM

1. REPORT NUMBER: AFOSR-TR-	2. GOVT ACCESSION NO.: AD-A142561
3. RECIPIENT'S CATALOG NUMBER:	
4. TITLE (and Subtitle): A laboratory study of aircraft precipitation static charging	5. TYPE OF REPORT & PERIOD COVERED: Final Report, 1 Aug 1982 - 31 Jul 1983
6. PERFORMING ORG. REPORT NUMBER:	
7. AUTHOR(s): Dr. A. J. Illingworth	8. CONTRACT OR GRANT NUMBER(s): AFOSR-82-0323
9. PERFORMING ORGANIZATION NAME AND ADDRESS: Department of Physics, Univ. of Manchester Institute of Science & Technology, Manchester M60 1QD, England	10. PROGRAM ELEMENT, PROJECT, TASK AREA & WORK UNIT NUMBERS: (61102F 2310/A1
11. CONTROLLING OFFICE NAME AND ADDRESS: Air Force Office of Scientific Research, Bolling AFB, Washington DC 20332 NC	12. REPORT DATE: May 1984 13. NUMBER OF PAGES: 50
14. MONITORING AGENCY NAME & ADDRESS(if different from Controlling Office): EOARD / LNG, Box 14, FPO New York 09510	15. SECURITY CLASS. (of this report): Unclassified 15a. DECLASSIFICATION/DOWNGRADING SCHEDULE

16. DISTRIBUTION STATEMENT (of this Report)

Approved for public release, Distribution unlimited

17. DISTRIBUTION STATEMENT (of the abstract entered in Block 20, if different from Report)

18. SUPPLEMENTARY NOTES

19. KEY WORDS (Continue on reverse side if necessary and identify by block number)

Precipitation static

20. ABSTRACT (Continue on reverse side if necessary and identify by block number)

Laboratory experiments show that when small ice particles collide with targets at speeds of up to 80m/s then the charge transfer is dependent upon the work function of the target material. Most common materials charge negatively, in agreement with observed aircraft charging in ice clouds, but magnesium which has a low work function charges positively. These results enable the charging of materials to be predicted before flight, and also suggest that alloys of magnesium should minimise aircraft charging. The laboratory apparatus could be used to characterise the charging of the new composite materials for aircraft surfaces.

DD FORM 1 JAN 73 1473 EDITION OF 1 NOV 65 IS OBSOLETE

UNCLASSIFIED

SECURITY CLASSIFICATION OF THIS PAGE (When Data Entered)

Table of Contents

1 - INTRODUCTION

There is a renewed interest in the subject of static charging of aircraft by precipitation, and three potential problems may be identified.

1) Microelectronics and digital systems are more prone to interference by transient pulses than are analog systems.

2) New composite and dielectric materials are being used on aircraft surfaces. They have lower conductivities than metals and may charge more rapidly when precipitation particles impact upon them.

3) Microelectronics are being increasingly used for flight control and generally in situations where any failure is potentially catastrophic.

This report describes laboratory work carried out at UMIST which gives considerable insight into the fundamental processes of charge flow and separation which operate when small ice particles impact upon metal surfaces. The experiments have shown that the charge transferred depends upon the work function of the metal surface. This finding has two important implications.

1) The charging properties of metallic surfaces can be predicted before they are flown.

2) Materials with low work functions and particularly magnesium charge positively; but most materials used for aircraft surfaces charge negatively. This is consistent with the observed negative charging of aircraft when flying through clouds containing ice crystals.

3) Intermediate alloys should exist which charge to a negligible extent.

We have not yet carried out an extensive series of tests on the charging of the new composite and dielectric materials. However, the existing apparatus which has been used for investigating the charge acquired by a metal target when an individual ice crystal impacts upon it at high speed, can be modified to characterise the charging properties of a range of targets fabricated from these new materials.

In Section 2 we describe the apparatus used for studying the high velocity collision of ice particles with various metallic targets. Section 3 presents the charging results, and in Section 4 the laboratory results are compared with the observed charging obtained from instrumented aircraft. The final Section 5 contains conclusions and suggestions for further work.

Further details may be found in the six appendices comprising papers published in refereed journals and presented at conferences. The first three are papers published during 1983 of work completed under AFOSR-81-0189, the fourth and fifth are papers to be presented at the VIIth International Conference in Atmospheric Electricity in Albany, June 1984, and submitted to the Journal of Geophysical Research. These first five papers deal with aspects of the conduction processes in ice and tests of the various charge separation hypotheses, with the conclusion that only the contact potential mechanism operates in situations of atmospheric relevance and that others may be rejected. These appendices describe in detail the experimental apparatus and results which enable the following mechanisms to be rejected: (a) the thermoelectric mechanism due to temperature difference, (b) the inductive effect i.e. charging due to an external field, and (c) freezing potentials due to contaminants in the ice. These experiments are not discussed further in Sections 2 and 3.

The sixth appendix, which is the paper to be presented at the 1984 International Aerospace & Ground Conference on Lightning and Static Electricity, in Orlando, Florida, June 1984, contains the major conclusion on the work function mechanism believed to operate when ice crystals collide with metal targets at aircraft speeds.

2 - APPARATUS

Figure 1 shows the apparatus for producing single ice particles of controllable size and charge and then accelerating the particles to a velocity of up to $80ms^{-1}$ before the collision with a target.

Water droplets in the size range 50 - 200μm with a controllable charge (0 to ± 250fC) were produced at the rate of about 1Hz by a droplet generator on top of the cold room. Each droplet then froze slowly as it fell down a tube into the cold room and collided with a tenuous cloud of minute ice crystals, which was formed by cooling a short section of the tube. The time for the particle to pass between two induction rings placed just below the freezing section then enabled the terminal velocity of each particle to be determined, and hence the size estimated to better than 10μm. After falling a further 45cm, sufficient for the 100μm particles to freeze completely and reach thermal equilibrium, the particles were accelerated to speeds of up to $80ms^{-1}$ by compressed air. The compressed air was introduced at the periphery of the tube between two co-axial cones with an adjustable separation of about 1mm. This symmetric conic jet served to centre and to accelerate the small ice particles. The accelerated ice particles then passed through a final induction ring before hitting the target. The target was a cylinder

(to follow p2)

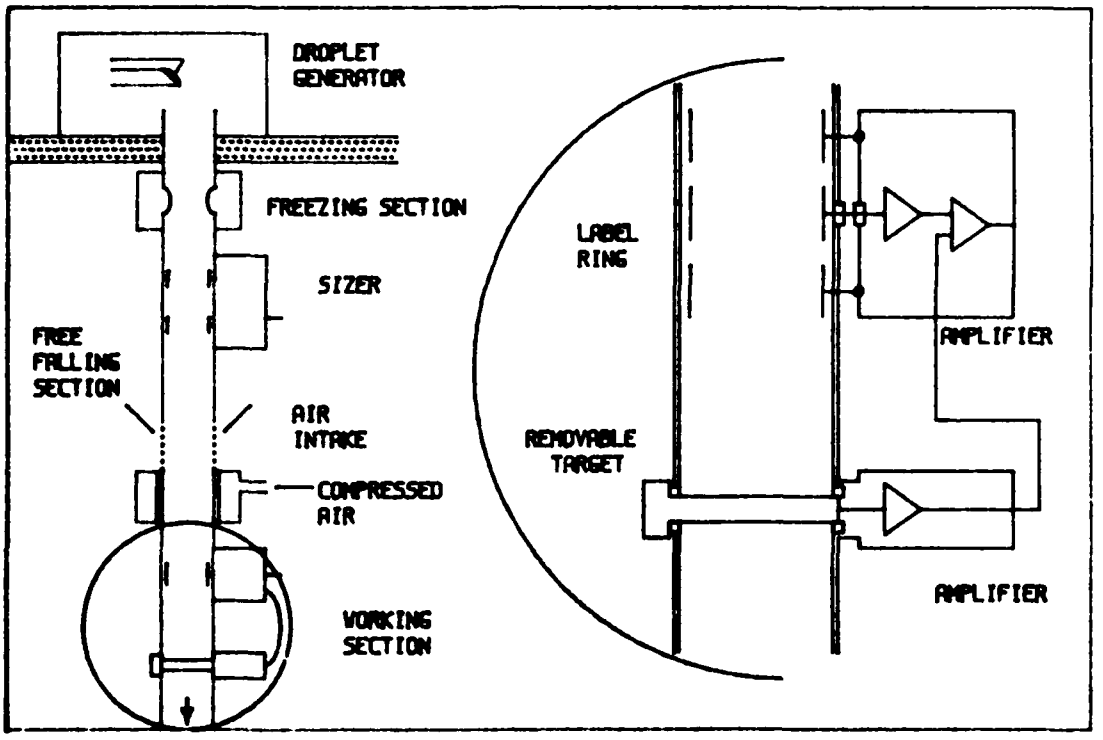

Fig 1: The apparatus for studying individual collisions of ice particles with various metal targets.Not to scale.

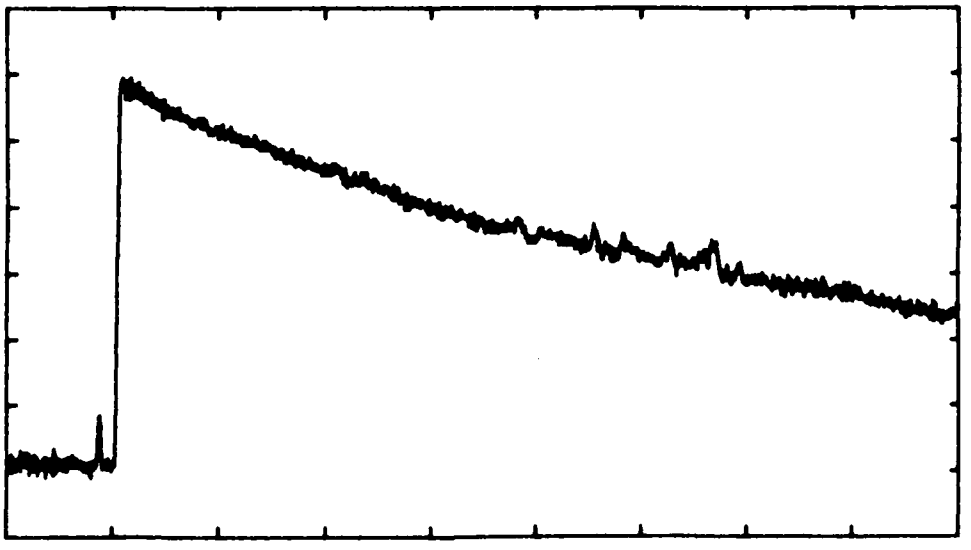

Fig 2: Positive charging when a 100um ice particle hits a magnesium target at 80m/s. Horizontal scale 10msec per division, vertical scale 200fC per division. Temperature $-10^{o}C$.

4mm in diameter and was easily removable so that the charging properties of different materials could be investigated.

Separate amplifiers were placed as close as possible to both the induction rings and the target to reduce microphonic and 50Hz pick up to the equivalent of less than 2fC. The amplifier outputs were summed, recorded, and subsequently replayed and examined on a digital storage oscilloscope. Because the amplifier has a rise time of 3μsecs but a long (100msec) decay time for any charge deposited on the target, it was possible to differentiate between the rapidly varying induced charges caused by approaching and departing charged particles, and the long 100msec exponential decay when charge was transferred to the target.

A typical charging event in which a magnesium target acquires positive charge is shown in Figure 2. This waveform has two features. As the ice particle passes through the induction ring just above the target its charge before collision (in this case + 120fC) is sensed and gives rise to the 'blip' on the waveform. It then hits the target, and transfers + 1200fC of charge to the target. Because a net transfer occurs to the target, the amplifier waveform decays with a 100 msec exponential time constant, and the charge transfer can easily be differentiated from the rapid rise and fall of the charge induced of the waveform. In this example, the two waveforms are separated by 1.5msec, and as the target is 12cm below the ring the impact velocity is calculated to be $80ms^{-1}$. Further discussion of possible charging waveforms is given in Appendix F.

The 4Mhz bandwidth of a commercial video recorder was used to record the charging waveform. A 2Mhz carrier was FM modulated by ± 40% using a phase locked loop. On playback and demodulation this gave an analogue bandwidth of 200 khz with a rise time of 3μsecs and a linearity of ± 2%. These waveforms were examined on a digital storage oscilloscope, and the digital information transferred to a small computer for analysis and plotting if required.

3 - EXPERIMENTAL RESULTS

In order to identify genuine events caused by ice particles of known size hitting the target and to measure the speed of impact, it was necessary to put a charge on the ice particle so that its presence was sensed by the induction ring above the target as shown in the waveform of Figure 2. Spurious charging events due to extraneous crystals or specks of dust would not give a pulse at the induction ring and so could be rejected.

(to follow p3)

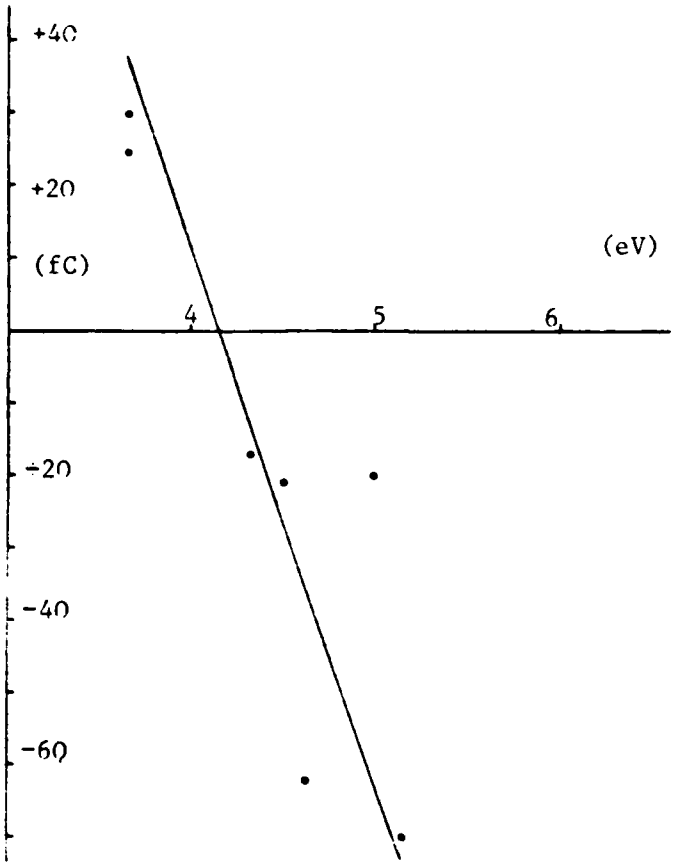

Fig 3: Average charge transfers to the target against work function of the target for magnesium, zinc, carbon, silver, and nickel.

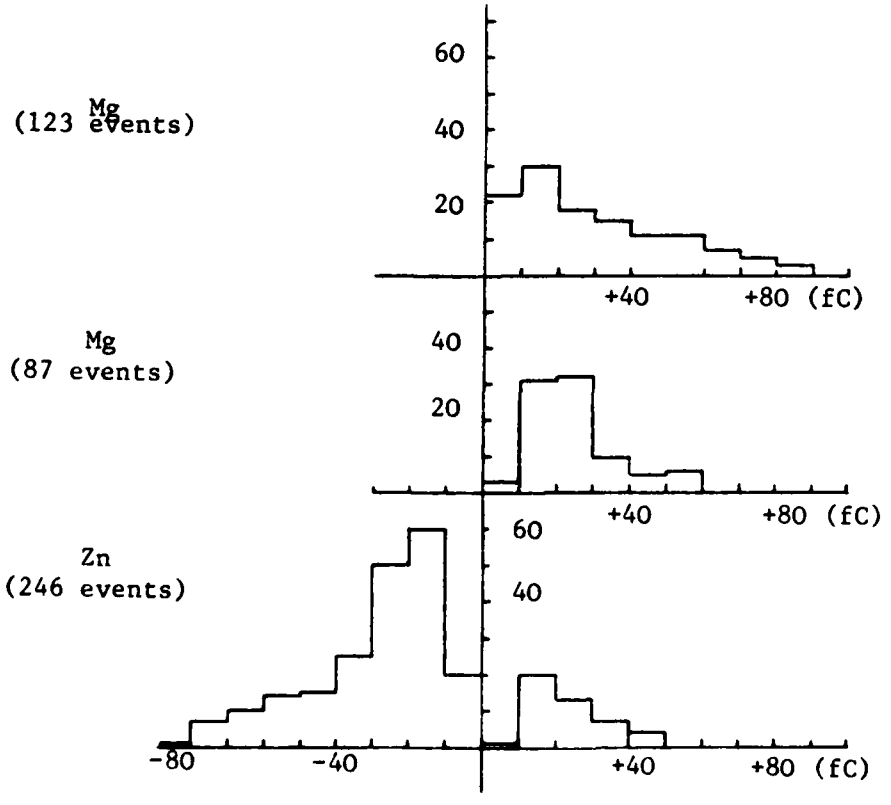

Fig 4: Histograms of charge transfers to magnesium and zinc targets.

(to follow p3)

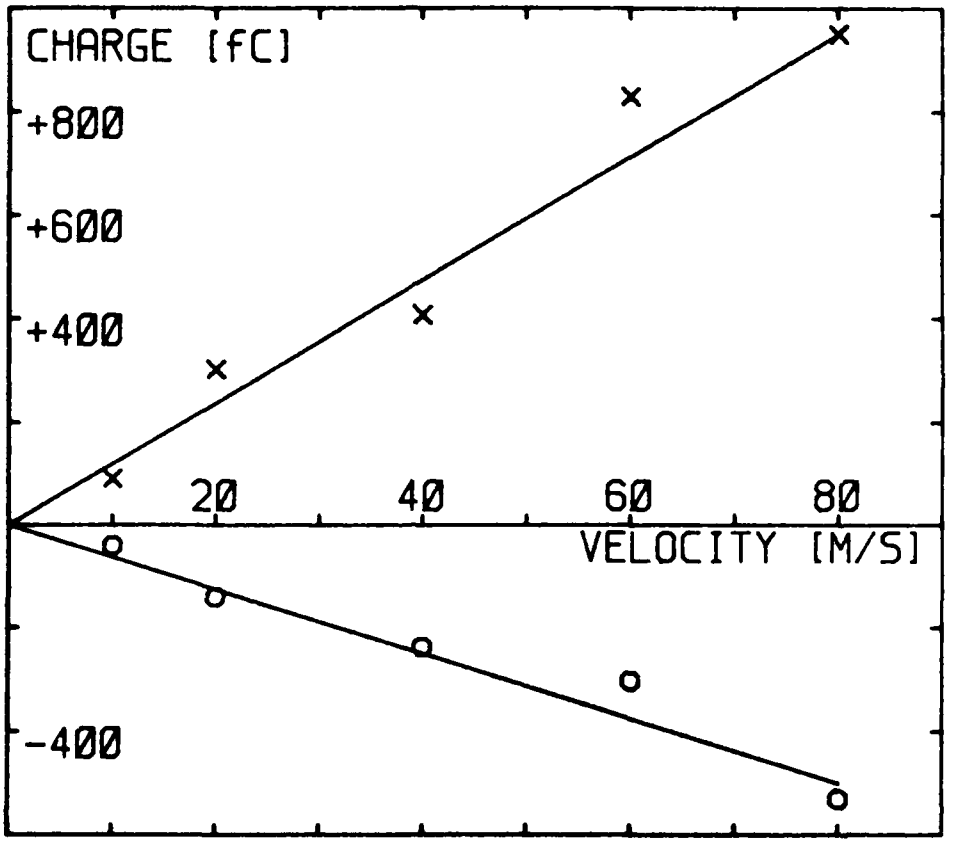

Fig 5 The charge transferred to magnesium (X) and nickel (o) targets as a function of velocity by 100um ice particles at $-10^{o}C$

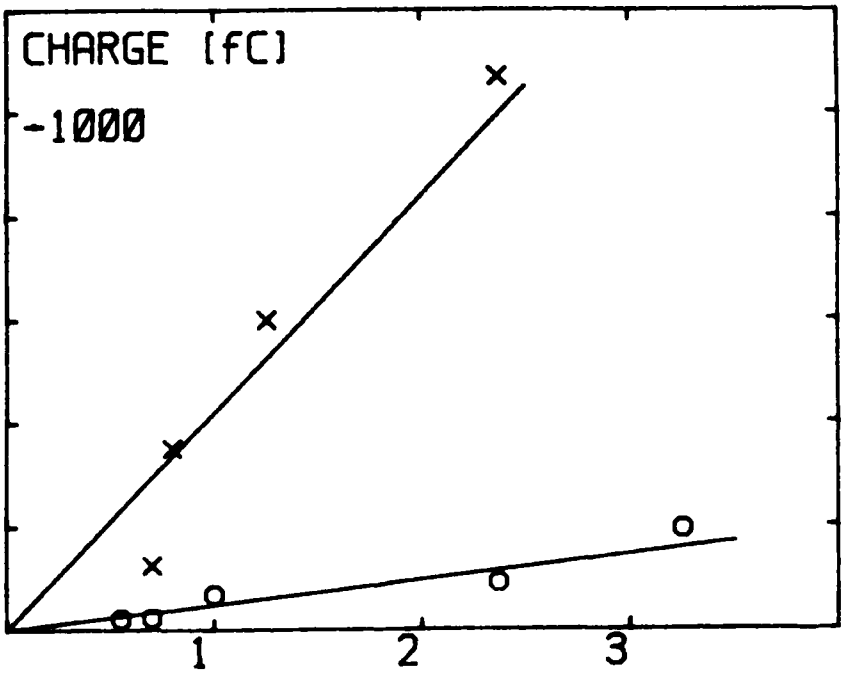

Fig 6: The charge acquired by a nickel target as a function of the size of the ice particle. X 60m/s $o_4 10_2$m/s
The units of the horizontal scale are $10^4 um^2$.

A series of experiments (Appendices B and D) confirmed that with the level of contaminants found in the atmosphere and used in these experiments, the surface conductivity of ice is so low that initial charge on the ice particle does not affect the charge transferred during the collision. In other words the initial charge may be considered as an identifying "label". The ice particles were made from water having a conductivity of less than $1.5\ 10^{-6}$ mho cm^{-1}. In all the experiments the temperature was kept at -10°C.

In Figure 3 the average charge transferred by 100μm ice particles impacting at $10ms^{-1}$ upon various metallic targets is plotted against the work function of the target. The values of work function were taken from the Handbook of Physics and Chemistry and so the actual values of the targets used may be slightly different and dependent upon the state of the surface. The individual charge transfers were quite variable, as shown by the histograms in Figure 4. This variability is probably due to different positions of the collision with the cylindrical target. All the points in Figure 3 are the average of at least 100 collisions, and demonstrate that the work function of the target is the principle parameter controlling the charge transfer. Particularly striking is the positive charging of the metal magnesium which has a low work function.

When the range of velocities was extended to those closer to aircraft speeds the work function still appears to be controlling the charge transfer. Figure 5 shows that the charging increases linearly with velocity up to $80ms^{-1}$, with magnesium charging increasingly positively over this range and nickel acquiring more negative charge as the velocity increases. In this Figure each point represents the average of at least 50 individual charge transfers.

In order to examine the effect of size on the charge transfer a series of experiments was performed using ice particles in the size range 75 to 220μm and a nickel target. For some of the interactions with the largest particles positive charging was found, and these events were often accompanied by complex waveforms. It appears that although the 45cm long free fall section of tube is long enough for complete freezing of the 100μm particles, because of the mass increase and greater terminal velocity, the 200μm particles are only partially frozen and so are likely to disintegrate when hitting the target.

Figure 6 displays the average charge transfer as a function of the square of the size of the ice particles for collision velocities of 10 and 60ms^{-1}. Data for sizes above 200μm have not been included because of the fragmentation problems discussed above. For the 10ms^{-1} run with 183μm particles about one third of the events resulted in positive charge transfer with an average value of 198fC, but only the two thirds which gave simple waveforms with negative charging have been included in the analysis. No positive events were observed for the other points shown on the graph. For the experiments of 60ms^{-1} the compressed air was interfering with the droplet generator and so some difficulty was experienced in keeping the droplet size constant and is responsible for the increased scatter. For both velocities, it is clear that the average charge transfer is increasing with velocity, and there is strong evidence for a square law dependence. A short experiment using 130μm supercooled liquid droplets at 60ms^{-1} with a nickel target confirmed positive charging for non-frozen particles with an average transfer of + 120fC.

A target of barium oxide, which has a low work function charged consistently positively at high speeds. Other materials including aluminium, carbon and silver charged negatively. When 100μm particles at 60ms^{-1} and a target of brass covered with polyurethane paint were used, an average transfer of -670fC wasmeasured, a teflon covered target resulted in an average value of -500fC, and a target covered with smooth ice also charged negatively but to a lesser degree.

The ice crystals occurring in the atmosphere are vapour grown and have different shape and momentum from the spherical particles used in this experiment. At the start of each experiment a cloud of minute ice crystals would form in the cooled section of the free fall tube, and this cloud would persist for a few minutes, and give rise to occasional clearly observable charging events when the crystals hit the target. Such events were not preceded by a recognisable label and so, because of the unknown size of the ice crystal, were not included in the analysis, however, the crystals always gave the same sign of charging as the controlled ice spheres. The low work function magnesium charged positively and the nickel acquired negative charge.

4 - COMPARISON WITH AIRCRAFT OBSERVATIONS

Aircraft generally acquire negative charge when they fly through clouds, as a result of the triboelectric or frictional charging occurring when water or ice particles in the cloud collide with the aircraft surface.

Tanner (1) has reported current densities for aircraft to be in the range 50-100μA m^{-2} for cirrus clouds, 100-200μA m^{-2} for stratocumulus, and 300μA m^{-2} for snow. Boulay and Laroche (2) measured the current to probes covered with conducting paint on a Meteor aircraft flying at 200 ms^{-1}, and confirmed these values. They estimated that the overall capturing area of the aircraft was about $8m^{+2}$, and calculated the maximum charging current to be 3mA, which compared well with the highest discharger current recorded of over 2mA. On only one occasion, in liquid precipitation near the ground, did they record positive current. In an investigation which extended to higher speeds, Nanevicz (3) also measured current in the range 100-200μA m^{-2}, but, in addition, observed the ice crystal concentration. At mach 1.2 he estimated that each ice crystal collision transferred about 50pC, the value was slightly higher at $200ms^{-1}$, but at mach 1.9 the charge per interaction was reduced by about 50%.

The negative charging found in this study with most common metals and paint covered targets is consistent with the negative charging observed with aircraft. Direct quantitative comparison of the laboratory studies with aircraft measurement involves an assumption of the typical size and concentration of ice particles in clouds. The charge per interaction for a 100μm particle has been found to be about -1pC at $80ms^{-1}$. From our derived velocity and size dependence this would suggest that a 200μm particle at $200ms^{-1}$ would charge to a target by about -10pC. If the concentration was 100 per liter then the current would be about 200μA m^{-2}, in agreement with most aircraft measurements. Boulay and Laroche (2) recorded one occasion of positive charging in rain, which is compatible with our findings with liquid drops. Nanevicz (3) found a charge per crystal of about -50pC at much higher velocities. It would be of interest to fly magnesium probes to see if they charged positively.

5 - CONCLUSIONS

The charging of metal targets by small ice particles increases linearly with velocity for speeds of up to at least $80ms^{-1}$, and is approximately proportional to the square of the particle size for spheres of diameter up to 200μm. These results imply that the charge transfer is proportional

to the contact area (A) predicted by elastic collision theory to vary as

$$A \propto v^{4/5} \quad r^2 \qquad (1)$$

where v is the velocity anc r the radius of the small particle. If the work function (or contact potential) difference between the metal and the ice is V, then the charge transfer should be given by

$$q = CV \qquad (2)$$

where C is the capacitance as the small particle separates from the target and is proportional to the contact area A in equation 1. The positive charging observed at the higher speeds in this paper by magnesium and barium oxide targets, and the negative charging for other targets with larger work functions indicate that the differences in contact potential are controlling the charge transfer of these higher speeds.

Partially frozen and liquid drops appear to charge targets positively; positive charging by splashing water drops at much lower speeds has been explained in terms of the disrupcion of the electric double layer (4).

Trinks and ter Haseborg (5) have carried out experiments with 20mm diameter ice projectiles to simulate the effect of hailstone charging. Such large particles were totally pulverised when they hit metal targets at speeds in the range 35 to 1000ms^{-1}. The targets acquired negative charges of up to 10pC per interaction, but the total number of these violent collisions in a cloud should be low. The charging of aircraft by ice crystals should be dominant, because they were present in much higher concentration.

We hope to be able to extend the studies to examine the charging of targets with speeds of up to 200ms^{-1} to see if the linear increase with velocity still holds, and to enable more direct comparison with the aircraft observations. If the positive charging of magnesium extends to these higher speeds, then by suitable choice of alloys there is a probability that static charging of aircraft can be reduced or minimised. We would also aim to examine the charging properties of the new composite materials now being used for advanced aircraft.

6 - REFERENCES

1. R.L. Tanner, et al., "Precipitation Charging and Corona-Generated Interference in Aircraft", Technical Report No. 73, Project No. 2494, Contract AF 19 (604) 3468, 1961.

2. J.L. Boulay and P. Laroche, "Aircraft Potential in Flight", Eighth Lightning and Static Electrification Conference, Fort-Worth, 1983.

3. J.E. Nanevicz, "Flight-Test Studies of Static Electrification on a Supersonic Aircraft", Lightning and Static Electrification Conference, Culham, 1975.

4. H. Trinks, and J.L. ter Haseborg, "Electric Charging by Impact of Hailstones and Raindrops", Eighth Lightning and Static Electrification Conference, Fort Worth, 1983.

5. Z. Levin and P. Hobbs, "Splashing of Water Drops on Solid and Wetted Surfaces", Phil. Trans. Roy Soc. A, 269, 555-585, 1971.

The Contact Potential of Rimed Ice

J. M. Caranti[†] and A. J. Illingworth*

Department of Physics, UMIST, Manchester M60 1QD, England *(Received: August 23, 1982)*

Measurements of the contact potential of polycrystalline ice by the Kelvin method could not detect any difference between the values for ice which was evaporating and for ice which was growing by condensation. Large persistent changes in contact potential of up to 400 mV were observed if the surface was rimed with supercooled droplets at −15 °C. These potentials are a surface effect and appear to be related to the disorder of the rapidly frozen water. They decay with times similar to those for mechanical relaxation. Contact potential differences between rimed hailstones and nonrimed ice crystals may be important in thunderstorm electrification.

1. Introduction

Many workers are of the opinion that the charge transferred when ice crystals collide with hailstones is responsible for the electrification of thunderstorms. However, laboratory experiments attempting to measure this charge transfer in simulated cloud conditions have yielded inconsistent and contradictory results. A significant advance was made by Buser and Aufdermauer[1] who found that for collisions of 20-μm diameter frozen ice spheres at −45 °C with metal surfaces the charge transfer was linearly dependent upon the work function of the metal target. Targets with low work functions charged positively and vice versa. When they used a target made of ice, it was possible to reverse the sign of the charge transfer by changing the state of the surface; if it was evaporating it acquired negative charge, but when it was growing with frost on the surface it charged positively. This sign change was consistent with Takahashi's[2] report that the "surface potential" (or "contact potential" as we shall call it) of evaporating ice was 0.2 V more negative than that of condensing ice.

In this paper we present further measurements of the contact potential of evaporating and condensing polycrystalline ice. Natural hailstones grow by riming as they collect supercooled cloud droplets so experiments were conducted on the change in contact potential when ice was exposed to supercooled droplets at various temperatures.[3]

2. Nomenclature

The work function of a metal is defined[4] as the amount of work necessary to extract an electron from the metal interior to just outside its surface, and if the metal is also charged the extra work to carry an electron to infinity is called the "surface potential". Nason and Fletcher[5] measured the work function of ice photoelectrically and obtained a value of 6.3 eV. Buser and Jaccard[6] used an indirect method, assuming the work function of ice to be the same as that of a metal that did not charge when in contact with ice, and found a value of 4.4 eV. This approach assumes the existence of surface states in ice, with which a metal can interchange electrons.

However, Lowell and Rose-Innes[4] noted that although intrinsic surface states can occur in covalent solids, for molecular ones like ice they are quite unlikely to exist or if they do, they will be very near the band gap border. If this is so, then these intrinsic surface levels could not explain the difference between the apparent work function and the photoelectric one. There is also the possibility that these surface states could be generated by the very presence of the metal in contact. In that case, this way of defining the meaning of contact potential of ice would be misleading from the point of view of ice–ice collisions.

In this paper the term "contact potential" between two pieces of ice or ice and metal will be understood as the potential difference measured by the Kelvin vibrating capacitor method. This contact potential is not necessarily related to the values of the Fermi levels or work functions of the ice because it is quite likely that the charges that will flow during contact will not be electrons.

A practical difficulty arises with ice in the Kelvin apparatus. An unknown potential will be set up at the metal–ice surface. However, if this interface is kept constant when the ice surface is changed then it will be possible to derive the change in contact potential between ice formed by different methods, although the absolute value of these potentials will be unknown.

3. Previous Work

Mazzega et al.[7] used the vibrating capacitor technique to measure the contact potential for single crystals of ice upon a gold lower electrode. They assumed that the changes in contact potential with temperature detected by the upper electrode were those at the air–ice boundary and that the ice–metal interface contribution remained constant. They reported that superposed upon a linear trend with temperature there was a term proportional to ln (−T), where T is the temperature in °C, and noted that the same temperature dependence was theoretically predicted by Fletcher[8] for the thickness of a disordered layer on the ice surface.

The Mazzega et al. experiment was carried out in equilibrium conditions with no growth or evaporation. Takahashi[9] used the same vibrating capacitor technique and found that when ice initially at −5 °C was cooled to −25 °C so that it grew by deposition, the contact potential first changed to positive values followed by a relatively large negative change of 200 mV. When the ice was returned to its original temperature and the frost allowed to evaporate,the contact potential returned to its original value, completing a hysteresis cycle in the potential–temperature graph. In an additional experiment at constant supersaturation, he found that the change in sign of con-

[†] On leave from IMAF, Lapida 854, 5000 Cordoba, Argentina.

(1) Buser, O.; Aufdermaur, A. N. In "Electrical Process in Atmospheres"; Steinkopt: Darmstadt, 1977.
(2) Takahashi, T. *J. Atmos. Sci.* **1973**, *30*, 1220–4.
(3) Caranti, J. M.; Illingworth, A. J. *Nature (London)* **1980**, *284*, 44–6.
(4) Lowell, J.; Rose-Innes, A. C. *Rep. Prog. Phys.* **1980**, *29*, 947–1023.
(5) Nason, D.; Flether, N. H. *J. Chem. Phys.* **1975**, *62*, 4444.
(6) Buser, O.; Jaccard, C. *J. Glaciol.* **1978**, *21*, 547–58.
(7) Mazzega, E.; et al. *J. Chem. Phys.* **1976**, *64*, 1028–31.
(8) Fletcher, N. H. In "Physics and Chemistry of Ice"; Royal Society of Canada: Ottawa, Canada, 1973; p 132.
(9) Takahashi, T. *J. Atmos. Sci.* **1970**, *27*, 453–62.

0022-3654/83/2087-4125$01.50/0

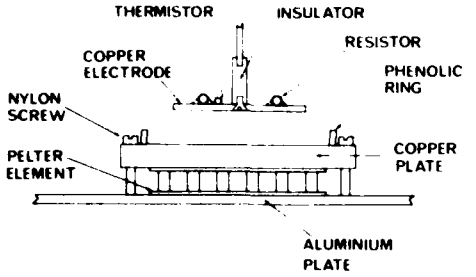

Figure 1. The lower electrode with sample holder and the solid upper vibrating electrode.

tact potential with time took place earilier at lower ice temperatures. This observation is somewhat puzzling since it shows that the ice contact potential depends on time as well as temperature, invalidating the precise correlation between potential and temperature implied in the first part of the experiment.

Takahashi[2] used a different approach, measuring the potential acquired by a copper sphere in a tube when ionized air passed around it, at the same time that ice is being grown on the surface. Starting with bare copper the sphere became positive as soon as ice appeared on its surface. Later, during evaporation, the potential changed to negative. Both values were approximately 100 mV. But from his graphs it can be seen that the potential during growth started to reverse sign long before (20 min) evaporation had really begun, suggesting that another process was going on at the same time. It has been pointed out[10] that differences in contact potential between tube and sphere could move ions of the appropriate sign to the sphere. Persistent and unpredictable potentials can be set up[11] when currents flow through a copper–ice interface.

4. Experimental Setup

The contact potentials were measured by the vibrating capacitor technique with the electrode arrangement shown in Figure 1. The lower electrode was a gold-plated copper block, placed above a Peltier thermoelectric element, which was itself mounted upon a more massive aluminum heat sink. The temperature of the electrode and ice sample upon it was controlled with a thermistor to vary the current through the Peltier element. The upper moving gold-plated electrode was attached to a vibrator through an insulating shaft; the whole assembly could be easily moved to allow access to the ice sample. Two other upper electrodes were also used. A gold-plated nickel mesh was employed when it was important to have an equilibrium vapor flux to the sample, and a solid electrode divided into two semicircles enabled changes in contact potential between different parts of the same ice sample to be measured. The temperature of the upper electrodes was controlled with a bead thermistor and heating resistors. All electrodes were about 40 mm in diameter and were vibrated up to 40 Hz, over this range no signal variation with frequency could be detected.

The signal from the upper electrode was connected to a current integrator which held it at virtual earth, and an automatic phase-sensitive nulling circuit applied a backing-off potential to the lower electrode to minimize the integrator output. This method has the advantage that the backing-off potential is a direct reading of the relative contact potential without needing any knowledge of electrode geometry, and it also minimizes any currents flowing to the electrodes and any consequent polarization problems

(10) Griffiths, R. F.; Vonnegut, B. *J. Atmos. Sci.* **1975**, *32*, 226–7.
(11) Hobbs, P. V. "Ice Physics"; Clarendon Press: Oxford, 1974.

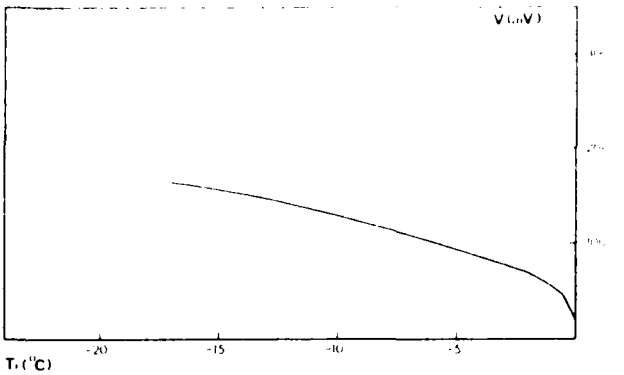

Figure 2. Contact potential variation for a constant air temperature of −11 °C and variable ice temperature (T_i). The two gold-plated electrodes alone gave 0 V.

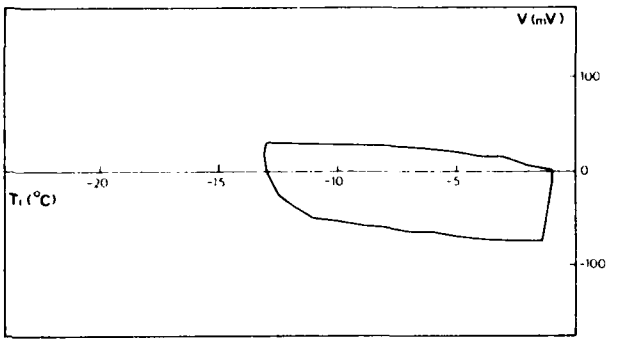

Figure 3. Hysteresis cycle caused by condensation on the gold upper electrode. The air temperature was constant at −8 °C and ice variable (T_i).

at the ice–metal interface. Cylindrical polycrystalline ice samples (diameter 50 mm and thickness 10–15 mm) were prepared by slowly freezing distilled water (10^{-6} mho cm^{-1}). The ice was then heated with a hot air blower and the wet sample placed on the lower electrode which was held just below 0 °C. This method of sample preparation produced crystals of about 1 mm diameter with negligible stress and ensured good electrical contact.

Preliminary experiments with copper electrodes showed that, when a potential of several volts was temporarily applied to the upper electrode, large spurious contact potentials were produced which persisted for several hours; these were probably due to rectification occurring at the copper–ice junction. With the gold-plated electrodes, after applying 500 V to the upper electrode (equivalent to a field of 5×10^5 V m^{-1} at the ice surface), a spurious nulling potential of about 100 mV persisted for only a few minutes.

5. Evaporation Deposition Measurements

Figure 2 shows variations of contact potential obtained when the temperature of the ice sample was changed but that of the cold room was kept constant at −11 °C and saturated with respect to ice. In this measurement the gold-plated upper electrode was solid and kept slightly warmer than the sample to prevent frost formation on it.

When the upper vibrating electrode was not heated, a completely different result was obtained. Figure 3 shows an example of a run taken with the gold-plated electrode. Even if the proximity to the sample prevented the electrode from reaching the air temperature, the same proximity helped the formation of frost without the need for large temperature differences as the sample acted as a supply of water vapor. When frost had covered the electrode surface the system behaved as if a vibrating ice electrode was being used instead of a gold-plated one. The

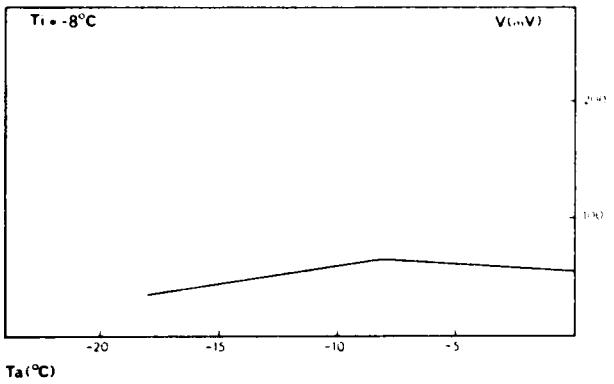

Figure 4. Contact potential variation during evaporation and/or deposition. Constant ice temperature −8 °C. Variable air temperature.

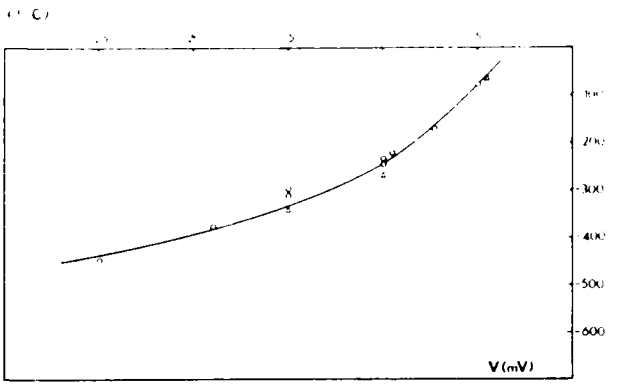

Figure 5. Riming contact potential changes as a function of temperature using the spinning top (triangles) and the spray generator (small circles).

effect can be seen in the sharp decrease in contact potential at the high temperature side of Figure 3, when the sample was evaporating and the electrode was condensing. The hysteresis arises because, once the frost has been formed, the new contact potential remained when the sample was cooled until the evaporation of the frost was complete.

It is interesting to note that a similar experiment using a solid copper upper electrode also gave a hysteresis curve, as ice formed and evaporated from it, but that the polarity of the change was opposite and larger than that of gold, and approximately the same value as that reported by Takahashi.[9]

The results in Figure 2 include any changes with temperature at the ice–metal junction, but this can be eliminated if the sample temperature is held constant and the air temperature varied. Figure 4 shows measurements made with a fixed air temperature of −8 °C with the permeable gold-plated upper electrode. There is no sign of the expected potential jump when the air temperature passes from the left side (evaporation) to the right side (condensation) although frost on the sample was clearly visible, but only a small slope at each side of about 1 or 2 mV/°C. Runs at different ice temperatures over the range −3 to −15 °C show the same characteristic slopes with similar gradients, in each case the maximum potential being recorded at the ice temperature. There is of course a shift in the dc level for runs at different ice temperatures due to changes at the ice–metal interface.

6. Discussion

It appears that hysteresis curves are associated with the growth and evaporation of frost from the upper electrode. When precautions were taken to avoid this, then no sudden step changes in contact potential could be detected when the ice sample changed from a state when it was evaporating to one with frost growing on the surface; but, as shown in Figure 4, only slow changes could be observed. In retrospect this is not surprising. The weight loss of a sample held at −12 °C and 55% humidity was measured and found to be equivalent to the loss of about two molecular layers per second. However, from kinetic theory considerations[12] the flux of molecules incident upon and leaving the ice surface in equilibrium is equivalent to about 7×10^5 molecular layers per second, so normal rates of evaporation or condensation will only represent negligible perturbations.

Results similar to those in Figure 4 were obtained over the range of ice temperatures −3 to −15 °C showing that although the crystal habit changed abruptly over this range there was no significant effect on contact potential. It is interesting to compare Figure 4, the changes in contact potential with temperature at the air–ice interface, with Figure 2 which also includes the contribution from temperature effects at the ice–metal junction. The shapes of the curves are quite different, thus showing that the analysis and conclusions of Mazzega et al.[7] which assumed the contact potential of the ice–metal interface to be invariant with temperature may be in error.

7. Contact Potential of Rimed Ice

The same electrode arrangement was used as previously, but in addition a 50 mm diameter thick wall aluminum tube 60 cm long was placed in the cold room above the ice sample. Supercooled droplets of distilled water were allowed to fall down this tube and freeze on the ice to form a rimed surface. Three methods of droplet production were used. A spinning top[13] gave 30–60 μm droplets, a spray produced 30-μm droplets, and an ultrasonic generator made larger 100-μm droplets. Consideration of the thermal inertia of the droplets[14] shows that after only 23 mm in free fall a 100-μm droplet has attained the ambient air temperature.

Negative changes in contact potential of up to 400 mV were observed when an ice surface was rimed; the temperature of the ice, electrode, and air was kept constant throughout. It was found that the change in contact potential saturated when the surface was completely covered with droplets. Once the limit was achieved, providing the temperature was unchanged, further riming did not alter the potential. For a partially covered surface, the upper electrode measured an intermediate value of potential.

Another crucial observation was that changes in potential caused by the landing and freezing of droplets on the ice substrate could be reversed by melting only the rime so formed and ensuring that the subsequent freezing occurred slowly. The temperature dependence of the riming potential is shown in Figure 5. Each point was obtained by subtracting the potential before riming from the contact potential after several layers of rime, therefore only changes brought about by the riming are shown, with no possible contribution from the ice–metal junction. After a reading was taken the surface was melted and the temperature adjusted to a new value. Droplets from the spray and the spinning top gave changes lying on the same reasonably well-defined curve and similar results were found for the larger droplets from the ultrasonic generator. It is clear from this graph that there is a tendency for the

(12) Pruppacher, H. R.; Klett, J. D. "Microphysics of Clouds and Precipitation"; Reidel: Dordrecht, Holland, 1978.

(13) May, K. R. *J. Sci. Instrum.* **1966**, *43*, 841.
(14) Kinzer, G. D.; Gunn, R. *J. Met.* **1951**, *8*, 71.

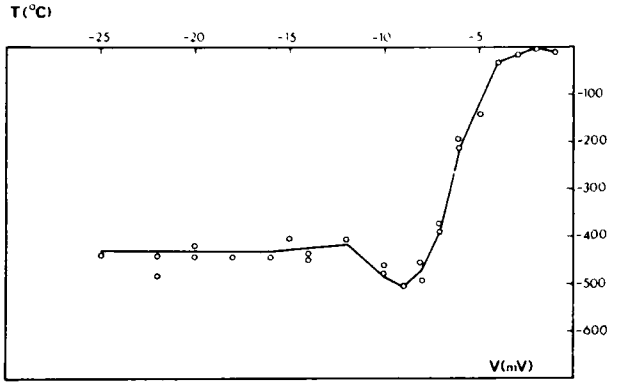

Figure 6. Contact potential of rime formed on an already rimed surface as a function of temperature.

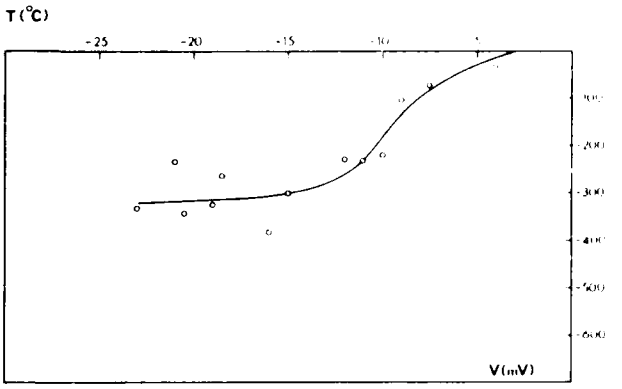

Figure 7. Contact potential changes of rime using the ultrasonic generator measured with the divided upper electrode.

rimed surface to be more negative than the bulk, and that with decreasing temperature the change tends toward a limit of the order of 0.5 V.

The melting of the rimed surface and later slow freezing produced a very smooth surface with which the droplets could exchange heat very efficiently. To study the effect on the contact potential of riming an already rimed surface, we made a set of measurements using the ultrasonic generator without melting between droplet layers. The result is represented in Figure 6, where compared to Figure 5 the riming potential reaches a maximum even earlier in the high-temperature region and falls to lower values at lower temperatures. The transition from wet growth, in which the surface remained wet and smooth rime was produced, to dry growth, with opaque bubbly ice being produced as each droplet froze before being covered by the next, occurred at about −10 °C and coincided with the maximum potential.

Because the change in potential does not seem to be cumulative, it appears that the change is associated with the surface. To check this we deposited successive layers of rime of total thickness 5 mm on the sample; when the last layer was melted by a very brief contact with a metal plate warmed to 20 °C, a partial return toward the original value of potential was observed, which is consistent with a surface effect.

To confirm that there was no possibility that the observed potential change arose from charged droplets landing on the surface and then becoming trapped as a blocking charge at the electrode interface, we contacted the surface for 5 s with a wire connected to 15-V power supply. Following disconnection there was an abrupt decay followed by a slower one, and after a few minutes the state was the same as before charging. An even more conclusive experiment, which also served to stress the importance of the surface in the riming potential, was when only half the ice sample was rimed with the ultrasonic generator. The split electrode described in section 3 was then used with one half sensing the contact potential of the rimed ice and the other the unchanged ice sample, and the differences in the two potentials are shown in Figure 7. If charge had accumulated then both halves would have been equally affected.

One of the most striking properties of the riming effect was its duration. When the sample was left overnight after riming, the value remained practically unaltered the next day. But after melting the surface, provided the temperature was the same, it returned to the potential it had before riming. It was also observed that this persistence was longer for lower temperatures. These decay times suggested that the riming effect was related to structural processes of ice probably grain boundary movements.

Another property was the memory effect. If the rime was made at a certain temperature and then changed to another, the potential remained the same, except for a temperature coefficient of about −7 mV/°C associated with the ice–metal junction. Using this property we measured the decay time as a function of temperature; for a 250-mV potential the initial slope was 7 mV/h at −3 °C and 1.7 mV/h at −12 °C.

8. Discussion on Riming Potentials

The lack of additivity of the potentials when successive layers of droplets were applied to the samples implies that the effect is not a bulk one which might arise if ice was piezoelectric, but that the potential jump resides on the surface. This idea is also supported by the reversibility of the change when only the surface of a thick layer of rime was melted and slowly refrozen. The different potentials sensed by the split electrode when only half of the sample was rimed provide further evidence of a surface effect.

The potential increased when the riming occurred at lower temperatures, and this suggests that the effect may result from rapid freezing. At these faster growth rates ice tends to become polycrystalline[15] and more line and point defects are formed; below −15 °C the crystal size tends to be smaller.[16] Levi et al.[17] found that between −10 and 15 °C there was a sudden increase in the probability of the rime having a different crystallographic orientation to that of the substrate.

The rate of freezing of the droplets is determined by the temperature of the ice substrate with ventilation and evaporation playing a secondary role.[18,19] The control the substrate has on the riming effect becomes apparent in the results of Figure 6. The transition from wet to dry growth occurring at around −10 °C causes the thermal conductivity of the substrate to decrease (as there was no melting between droplet layers) and at the same time the riming potential is observed to take lower values.

An independent experiment was carried out to check the freezing speed. Using very small quantitites of very hot air so as not to affect the rest of the ice, we melted the sample surface at various temperatures and immediately froze it with a strong jet of cold air at ambient temperature. Part of the liquid film was ejected and a very thin layer froze very fast. The contact potential change so produced was almost the same as the rime effect. As there was an

(15) Hallett, J. *J. Atmos. Sci.* **1964**, *21*, 671.
(16) Levi, L.; Aufdermaur, A. N. *J. Atmos. Sci.* **1970**, *27*, 443.
(17) Levi, L.; et al. *J. Cryst. Growth* **1980**, *48*, 121.
(18) Brownscombe, J. L.; Hallett, J. *Q. J. R. Meteorol. Soc.* **1967**, *93*, 455–74.
(19) Macklin, W. C.; Payne, G. S. *Q. J. R. Meteorol. Soc.* **1968**, *94*, 167–75.

interaction only with the surface, this implied that the potential jump resided on it and that the freezing rate was the dominant factor. The same dependence on freezing speed can explain why the riming effect can be reversed by melting the rimed surface and allowing it to refreeze slowly.

The most obvious result of rapid freezing is an increase in the disorder in the rime. The study of the decay times of the potential shows that they are similar to the times for mechanical processes such as creep rate.[20,21] In Fletcher's[8] model of the surface of ice a double layer arises as a result of a balance between the free energy lowered by the alignment of surface molecules and the entropy penalty due to the orientation. If rapid freezing causes an increase in the number of broken bonds a new balance should be obtained with more dipoles aligned on the surface causing a larger potential jump at the surface. As the ice recrystallizes the number of defects will fall and in equilibrium less dipoles should align at the surface, the time constant for the process being similar to that for mechanical relaxation.

9. Effects of Impurities, Rubbing, Evaporation, and Condensation on the Contact Potential of Rime

It is well-known that impurities affect the mechanical and electrical properties of ice. Experiments were carried out with NH_3 and HF, which are proton donor and acceptor, respectively, and enter the crystalline structure as substitutional defects. NaCl was also used because of its atmospheric incidence.

The solutions had concentrations ranging from 10^{-2} to 10^{-5} M and the droplets were in general produced with a solution of the same concentration as that of the sample. So that a noticeable change in the riming potential could be obtained, concentrations as high as 10^{-2} M were needed for NaCl, which then gave only 70 mV at −10 °C with a decay time as short as 0.5 h. NH_3 at 1.6×10^{-2} M could not be resolved, in magnitude and decay time, from distilled water. On the other hand, HF, at the same concentration, produced a more erratic effect with decay times of 1 h. When the concentration of these impurities was reduced to values just above those of cloud physics interest, the behavior for all of them was practically the same as distilled water except for the decay times, which at −12 °C and 1.6×10^{-4} M for NaCl, HF, and NH_3 were 4, 7, and 24 h, respectively. When rain water with a conductivity of 55 μmho/cm was also used, at low temperature it gave a riming potential about 20% larger than distilled water.

The influence of dissolved gases in the water used to make the rime was also studied as they should affect the concentration of bubbles formed in the ice. In one case the water was boiled and then sealed while cooling before being used for riming, and at the other extreme water saturated with oxygen was used, but no effect on riming potentials could be detected.

So that the effect of rubbing could be studied, an unrimed ice surface was planed with the blade of a sharp knife and negative changes in contact potential of 200 to 300 mV were measured agreeing with Takahashi.[22] If the planing was done on one half of the sample, the split electrode detected these changes in the same way as for riming, which shows that the ice did not acquire a net charge in the process. The potential change by rubbing had as long a persistence as the riming one.

Finally, the effect of evaporation and frost was also considered. Condensation did not affect the riming potential. Large crystals several millimeters in length were grown on top of a rimed surface but the effect was negligible. In another experiment, rime was made on top of these crystals with the surprising result that no additivity was found. On the other hand, evaporation had the effect of accelerating the decay. In an experiment the sample was kept at −11 °C and the environment at −17 °C with an average humidity of 46%. In this situation the riming potential decayed exponentially, the initial slope giving a time constant of 68 min. A measurement of evaporation decay for a surface that was melted and blown with cold air gave similar values.

10. Discussion of Impurities, Rubbing, Evaporation, and Frost Effects

The levels of contamination expected in the atmosphere produced no significant change in the magnitude of the riming potentials. However, the observed decay of the contact potential with impurities supports the hypothesis of a link with the mechanical properties of ice. Measurements[23] of deformation of ice have shown that the creep rate of ice at −20 °C containing about 3×10^{-3} M HF was five times more than that of pure ice. In contrast, NH_3 showed a slight hardening. This means that HF-doped ice should relax mechanical stress faster than NH_3-doped or pure ice, and this is precisely the observation made in the experiment where for 10^{-4} M solutions HF decay time was 3.4 times less than NH_3. The stresses considered in this discussion relax through the movement of dislocations and grain boundaries and Glen[24] showed that HF-doped ice has many L defects which facilitate the dislocation movement.

Rubbing is known to produce dislocations and defects. The potentials produced by rubbing and riming decayed with a similar time constant, thus it seems plausible that they may both decay by the movement of defects. It is difficult to explain the origin of the rubbing potentials qualitatively. If the theory[22] is to predict the observed 300-mV change then the assumed number of defects produced must be increased by four orders of magnitude which seems unrealistic.

The frost grown on a rimed surface acted transparently for the riming contact potential probably because the new crystals grew without disturbing the underlying disordered structure. A likely explanation for the lack of additivity when rime was formed on vapor grown crystals, which in turn grew on a previously rimed substrate, is that some water could penetrate the open structure of the frost and affect the underlying rime.

The rapid decay of the rime effect with evaporation can be used to estimate the thickness of the disordered surface layer of rime. If the value of about 2 molecular layers evaporated per second measured in section 6 and a lattice parameter of 2.76 Å are used, then in 68 min a layer 2 μm thick should have evaporated. This value is three orders deeper than the surface layer calculated by Fletcher[8] and twenty times the experimental value of Golecki and Jaccard.[25]

11. Conclusion

No difference in the contact potential of evaporating and condensing ice could be found, but a large change was measured when the surface was rimed. It appears that this

(20) Steinemann, S. IASH General Assembly, Rome, 1954.
(21) Glenn, J. W., *Proc. R. Soc. London, Ser. A* **1955**, *228*, 519.
(22) Takahashi, T. *J. Atmos. Sci.* **1969**, *26*, 1259–65.
(23) Jones, S. J.; Glenn, J. W. *Phil. Mag.* **1969**, *19*, 13–24.
(24) Glenn, J. W. *Phys. Cond. Matter* **1968**, *7*, 43–51.
(25) Golecki, I.; Jaccard, C. *Phys. Lett. A* **1977**, *63*, 374–6.

change is a result of the disordered ice produced by rapid freezing of supercooled water, since the change is proportional to the rate of freezing and it relaxes with times comparable to those for mechanical relaxation. There is considerable evidence for a noncrystalline "liquidlike" layer on the surface of ice with some degree of dipole alignment permitted. It seems plausible that in a highly disordered ice surface with many defects it will be energetically favorable for more dipoles to align thus producing the more negative contact potentials observed. Further work on the surface properties of rimed ice would confirm this suggestion.

Armed with a knowledge of the variation of the contact potential of rime with the temperature of formation we find it is now possible to reinterpret many of the recent laboratory experiments[26-28] on charge transfer between colliding ice particles in a more consistent manner. Although some aspects cannot be quantified (for example, the positive charging of frost surfaces and the dependence on impurities), the charge transfer can usually be predicted by considering the difference in contact potentials between ice formed in different ways and the capacitance when the colliding particles separate. If collisions between ice crystals and hailstones are responsible for the electrification of thunderstorms then the assymetry causing the charge transfer could be more negative contact potential of the rimed surface of the hailstone.

Acknowledgment. This work was performed with the help of a scholarship from the CONICET, Buenos Aires, Argentina, and further financial support from Grant AFOSR 81-0189.

Registry No. Water, 7732-18-5.

(26) Takahashi, T. *J. Atmos. Sci.* **1978**, *35*, 1536–48.
(27) Gaskell, W.; Illingworth, A. J., *Q J. R. Meterol. Soc.* **1980**, *106*, 841–54.
(28) Jayaratne, R.; Hallett, J.; Saunders, C. P. R. *Q. J. R. Meterol. Soc.*, accepted for publication.

Reprinted from The Journal of Physical Chemistry, 1983, 87, 4078.

Frequency Dependence of the Surface Conductivity of Ice

J. M. Caranti[†] and A. J. Illingworth*

Department of Physics, UMIST, Manchester M60 1QD, England *(Received: August 23, 1982; In Final Form: March 17, 1983)*

Measurements of the surface conductivity of polycrystalline ice over the frequency range 0.1 Hz to 30 kHz and for temperatures from −3 to −15 °C show that the conduction cannot be explained in terms of a single Debye relaxation. The behavior is similar to that of amorphous semiconductors and lends support to Fletcher's theory of a disordered noncrystalline layer on the ice surface. The surface currents were predominantly real. Modifying the surface of the ice by riming, rubbing, or allowing frost to grow decreased the dc surface conductivity, but had a smaller effect on the ac response. Ice doped with 10^{-3} and 10^{-4} M NaCl showed a power law response over the complete frequency range with an exponent 0.2. Implications for the inductive theory of thunderstorm electrification are discussed.

Introduction

The high dc surface conductivity of ice provides the most direct evidence for the existence of an anomalous crystal structure at the ice surface.[1] To obtain further information on the nature of this surface, we performed a study of the frequency dependence of the surface conductivity. These data may also be of importance is assessing the validity of the inductive theory of thunderstorm electrification. If this mechanism is to operate, then when ice crystals collide with hailstones in an electric field, the polarization charges induced by the field on the surface of the hailstone must be able to flow along the hail surface on to the crystal, and this must happen in a time comparable with the contact time of the collision.[2] For ice particles of atmospheric importance the surface conductivity will dominate, and because contact times are so short ac conductivity data are needed. Measurements of the surface conductivity of ice by using guard rings (summarized by Hobbs[1]) give a value of 10^{-10} mho for single

[†]On leave from IMAF, Lapida 854, 5000 Cordoba, Argentina.

(1) Hobbs, P. V. "Ice Physics"; Clarendon Press: Oxford, 1974.
(2) Gaskell, W. *Q. J. R. Meterol. Soc.* **1981**, *106*, 841–54.

0022-3654/83/2087-4078$01.50/0

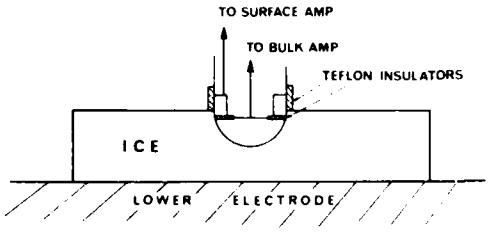

Figure 1. Electrodes for measuring the bulk and surface conductivities of ice.

crystals at −10 °C with an activation energy of 1 eV derived from the variation with temperature. Camp et al.[3] found a conductivity nearer 10^{-8} mho for polycrystalline ice at this temperature but with a similar value for the activation energy.

In this paper measurements are presented of the frequency variation of the real and imaginary surface conductivity of polycrystalline ice. The effect of modifying the surface was assessed, and the bulk conductance was also monitored in order to have a full picture of the changes brought about by riming, rubbing, and frost deposit on the surface. To enable comparison with laboratory experiments[4] which have tested the inductive theory by measuring the charge transfer between colliding ice particles in an electric field, we also investigated the conductivity of ice doped with 10^{-3} and 10^{-4} M NaCl.

Apparatus

The standard parallel-plate capacitor arrangement with guard ring is the most appropriate geometry for measuring the bulk currents in an ice sample. The currents to the guard ring are predominantly confined to the surface, but there is always a finite contribution detected which is flowing close to the surface but through the bulk. The arrangement in Figure 1 was devised to allow easy access to the surface while at the same time separating the bulk and surface currents. The lower electrode was a gold-plated copper block mounted upon a Peltier element for temperature control. A polycrystalline ice sample with crystal sizes up to 1 cm was prepared by slowly freezing cylindrical samples (diameter 60 mm, thickness 12 mm) generally of distilled water (10^{-6} mho cm^{-1}). The sample was warmed with hot air and the wet sample placed on the lower electrode which was held just below 0 °C, thus ensuring good reproducible electrical contact but with a minimum of stress within the ice. The upper electrode assembly comprised two parts, both made of gold-plated brass. One part, for sensing the bulk currents, was a hemisphere of 6.5 mm radius at the end of a cylinder. The surface electrode was a 6.5-mm radius ring placed just above the hemisphere and insulated from it by a thin sheet of Teflon. So that this composite electrode could be introduced into the ice a special drill bit was made which excavated a hemispherical hole in the ice sample. A water drop was placed in the hole and the electrode pressed into position. A Teflon sheath around the surface electrode left a width of less than 1 mm of the ring exposed (this particular dimension is not to scale in Figure 1) and ensured that the exposed part of the ring coincided with the surface of the ice.

Modeling with conductivity paper showed that the field distribution between the bulk electrode and the lower planar electrode was very similar to that given by the analytic solution for the bulk electrode and its electrostatic image. To derive a conductivity and dielectric constant from the bulk currents, we measured the capacitance between the hemisphere and the plane electrode. The surface resistance is given by

$$R = (\sigma_s(2\pi))^{-1}(\ln(a/b) + h/a)$$

where a is the sample radius and h its height, b the radius of the electrode, and σ_s the surface conductivity. This resistance can be considered as the resistance of the circular and vertical faces in series; consequently, when the state of the circular face was altered the change in its surface conductivity could be derived from the overall resistance change.

A sinusoidal voltage was applied to the lower electrode and currents to the upper electrodes were detected with FET op-amps in the current-to-voltage configuration. This arrangement has the advantage of holding the upper electrodes at virtual earth. To achieve a frequency response from 0.1 Hz to 200 kHz we placed this preamplifier as close as possible to the ice sample. The output of the preamplifier was connected to a voltage amplifier whose gain was switched between +1, when the phase of the voltage applied to the ice was from 0 to 180°, and −1 when the phase was 180 to 360°. The average dc output from this phase-sensitive detector was then proportional to the real current through the ice sample. A similar arrangement which switched the gain for phases 90 to 270° and 270 to 450° gave the imaginary current. Tests with artificial capacitances and resistances confirmed that the circuit operated up to 50 kHz. The frequency of the applied voltage was swept automatically and plots were obtained on an X–Y recorder of the variation of the real and imaginary currents against frequency.

The experiments were carried out over a range of temperatures from −1.5 to −20 °C. These temperatures were sensed by using a thermistor, which, combined with linearizing circuitry, enabled automatic plotting of temperature against conductivity. The thermistor was also used to control the current through the Peltier element thus enabling the temperature of the ice sample to be held a few degrees warmer or colder than the environmental air temperature.

Results

Preliminary measurements over the frequency range 0.1 Hz to 50 kHz demonstrated that the currents through the ice varied linearly with voltage for values of up to 15 V, thus indicating that they were not being affected by any blocking charges at the electrodes. Consequently, in all the experiments a peak-to-peak value of π volts was applied to the ice, as this gave a 1 V output when applied directly to the phase-sensitive detector circuit.

Over the temperature range studied the actual current detected by the surface electrode always exceeded that of the bulk for frequencies below a few hundred hertz. Typical measurements of the variation with frequency of the surface and bulk real conductivities for a sample of pure polycrystalline ice at −10 °C are shown in Figure 2, and differences in the behavior of the surface and the bulk are immediately apparent. Whereas the bulk shows the familiar S shape near frequencies of a few kilohertz expected from the Debye relaxation and its CR equivalent circuit,[5] this response is totally absent for the surface conductivity. At higher frequencies the bulk conductivity tends to a constant value, but the surface conductivity continues to rise. Further measurements showed that this trend continued up to 50 kHz.

When the data in Figure 2 are taken together with the imaginary component and a Cole–Cole plot of the real (ϵ')

(3) Camp, P. R. et al. In "Physics of Ice"; Plenum: New York, 1969.
(4) Caranti, J. M. Ph.D. Thesis, UMIST Manchester, England, 1982.

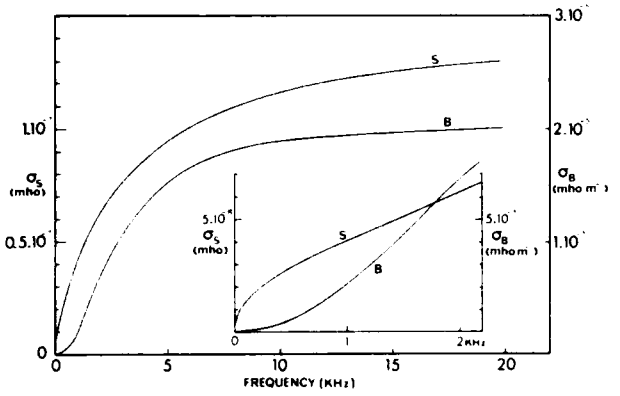

Figure 2. The real part of the surface (S) and the bulk (B) conductivities (σ) as a function of frequency for a sample of polycrystalline pure ice at −10 °C.

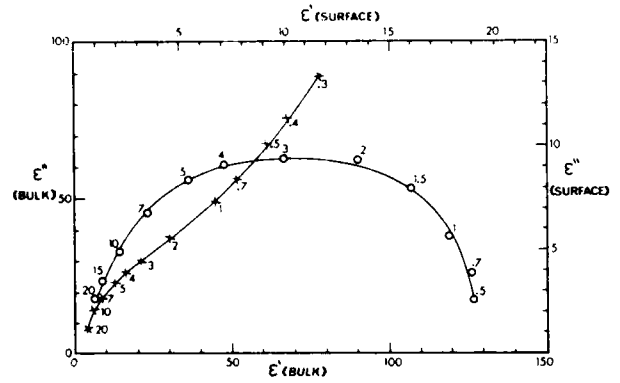

Figure 3. Cole–Cole plot for ice sample at −10 °C: bulk, O; surface, ×. The real (ϵ') and imaginary (ϵ'') dielectric constant are absolute values for the bulk, but in arbitrary units for the surface. Numbers beside the points are the frequencies in kilohertz.

and imaginary (ϵ'') dielectric constant is made for the bulk, then, as displayed in Figure 3, the points for various frequencies lie on a semicircle. This is the behavior expected for a substance obeying the Debye equations; the maximum value of ϵ'' indicating a dispersion frequency of about 3 kHz. The center of the semicircle is slightly below the real axis suggesting a small spread of dispersion frequencies within the bulk.[5] Because ϵ'' is derived by dividing the measured current by the frequency, then the noise in the front-end current-to-voltage amplifier rendered values of ϵ'' unreliable below 400 Hz.

It is impossible to define a dielectric constant for the surface without assuming a value for the depth of the conducting layer; however, for comparison purposes, Figure 3 also includes (in arbitrary units) the real and imaginary surface conductivites divided by the frequency, which are an equivalent imaginary and real dielectric constant, respectively. The surface behavior is totally different from the semicircle shown by the bulk, and if an analytic description is at all possible, then it is closer to a straight line. The phase angle is always small, showing surface currents to be predominantly resistive. We can see from Figure 2 that the deviation from the semicircle cannot be explained in terms of low-frequency branching due to the dc component of the surface conductivity; first, as the frequency rises the dc component soon becomes a small fraction of the total, and, second, the inset to Figure 2 emphasizes the difference in the shape of the two conductivity curves.

(5) Bottcher, C. J. F.; Bordewijk, P. "Theory of Electric Polarisation"; Elsevier: Amsterdam, 1978; Vol. II.

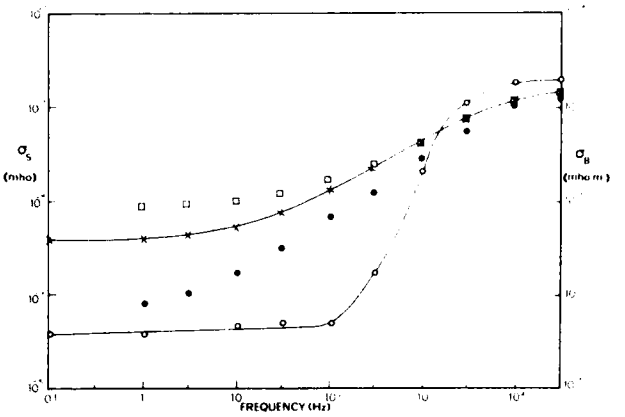

Figure 4. The variation of the real part of the conductivity with frequency for pure polycrystalline ice at −10 °C: O, bulk (σ_B); ×, surface (σ_s); ●, surface with thick frost; □, surface after annealing.

To demonstrate the behavior over the frequency range 0.1 Hz to 30 kHz more clearly, we present log–log plots of the real conductivities against frequency in Figure 4. The bulk real conductivity is low and steady up to 100 Hz, but then rises by over two orders of magnitude between 100 Hz and 10 kHz, in agreement with the predictions of Debye relaxation. The surface conductivity shows a more gradual rise extending over a much greater frequency range; although from 0.1 to 10 Hz the value only rises slightly, from 10 Hz to 10 kHz the slope is steeper and reasonably constant with a gradient of about 0.5.

For the ice sample in Figures 2–4 at −10 °C the extrapolated dc real surface conductivity had a value of about 5×10^{-9} mho and the bulk conductivity was about 5×10^{-8} mho m^{-1}, although this latter value is only correct to 25% because of amplifier noise. When different samples were prepared the conductivities were not identical. The changes in the bulk values could be accounted for by uncertainties in the separation of the hemispherical and lower planar electrode, but the absolute values of the surface conductivity varied by up to a factor of two.

The sensitivity of the surface is further demonstrated in Figure 4. If the ice sample was held below the dew point of the cold room by the Peltier element so that a thick (>1 mm) layer of frost formed, then, measured at constant ice temperature, the low-frequency real surface conductivity fell by a factor of five, but the fractional change in the high-frequency value was much less. The figure also shows that annealing the surface, by successively melting and slowly refreezing it, doubled the low-frequency surface conductivity. In contrast, a natural hailstone grows by riming as it collects supercooled water droplets which freeze rapidly on impact with the hail. When supercooled droplets of about 30 μm diameter were allowed to fall on the surface then there was a large reduction in the 10-Hz real surface conductivity. For example, when pure ice at −10.5 °C was used it fell about fivefold. At higher tempertures the change brought about by riming was less marked; at −3.5 °C the fall was only 12%, but at −15 °C the reduction was at least one order of magnitude. These conductivity changes resulting from riming persisted for hours but we have not yet carried out a detailed study of decay times. If the rimed surface was melted and allowed to refreeze slowly, then the conductivity returned to a value close to the original one. To check that this reduction due to riming was not simply a result of the surface geometry of nonisotropic rime, we melted the surface and then rapidly froze it with a jet of cold air; smooth ice was formed and a noticeable reduction of conductivity was observed.

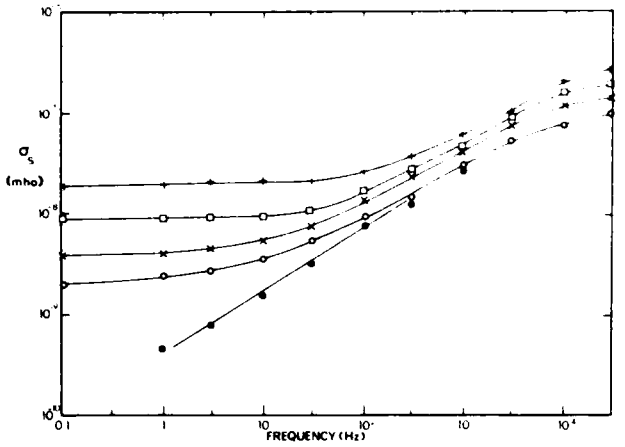

Figure 5. The frequency variation of the real part of the surface conductivity of pure polycrystalline ice: +, −3 °C; □, −7 °C; x, −10 °C; O, −15 °C; ●, −15 °C (ac component only).

but the effect was not so reproducible as the rime itself. Rubbing the surface was very effective in lowering the surface conductivity of pure ice even at high temperature; for example, at −3.5 °C it fell by a factor of five when shaved in several random directions with the blade of a sharp knife.

Although frost, annealing, riming, and scratching had a dramatic effect on the real dc surface conductivity no change in the bulk currents was observed. There were small changes in the imaginary component of the surface conductivity when the surface was modified, but these were less than a quarter of the changes of the real component, lending further support to the idea that the currents in the surface itself are predominantly resistive.

The frequency dependence of the real surface conductivity at different temperatures from −3 to −15 °C is shown in Figure 5. The temperature has a larger effect on the low-frequency response; below 300 Hz at −3 °C the conductivity is virtually constant, but at −15 °C the conductivity is still slowly falling with decreasing frequency at 0.1 Hz. The changes with temperature at higher frequencies were proportionally very much less. In order to facilitate comparison with work on other materials[6] we also include a plot of the ac component (obtained by substracting the 0.1-Hz contribution). For clarity only the −15 °C ac results are plotted in the diagram; the ac response follows a power law over the range 1 Hz to 1 kHz with a gradient of 0.65.

An Arrhenius plot of the 10-Hz real surface conductivity against reciprocal temperature is shown in Figure 6. For pure polycrystalline ice the gradient gives an activation energy of 1.0 eV, in good agreement with Camp et al.[3] The energy derived from the 0.1-Hz data is not significantly different. When the surface was modified, as described previously, the absolute values of the surface conductivity changed, but no alteration in the activation energy could be detected. Experiments were carried out on ice doped with 10^{-3} and 10^{-4} M NaCl and the values of the real surface conductivity at 10 Hz for various temperatures are also included in Figure 6. The slopes are less than for pure ice with estimated activation energies of 0.68 eV for 10^{-4} M NaCl and 0.55 eV for 10^{-3} M NaCl. The absolute values for doped ice may be affected by evaporation concentrating contaminants in the surface; however, a similar large reduction in energy has been reported[7] for single crystals

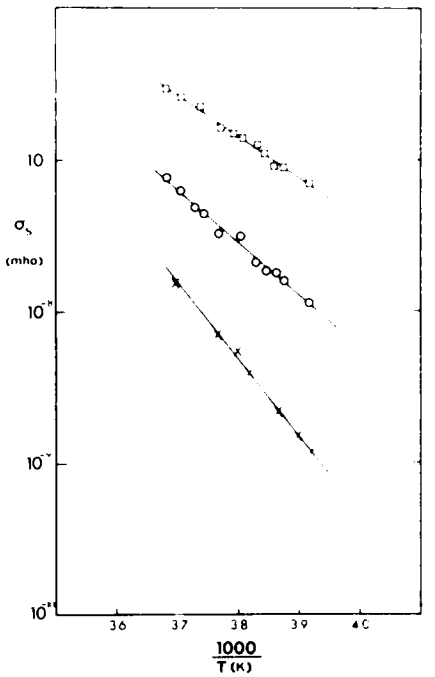

Figure 6. Arrhenius plot of the 10-Hz real surface conductivity: ×, pure ice; O, 10^{-4} M NaCl ice; □, 10^{-3} M NaCl ice.

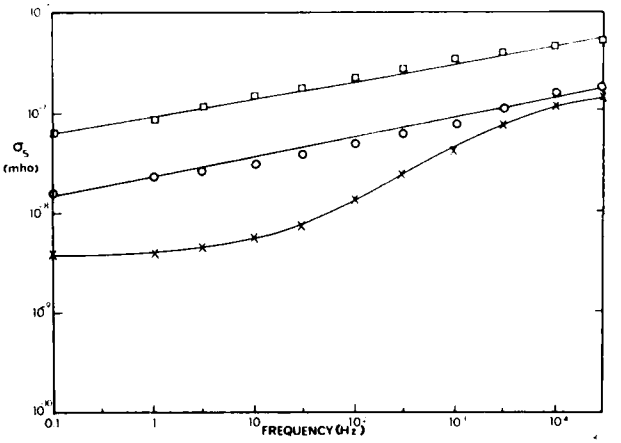

Figure 7. Variation of the real surface conductivity of polycrystalline ice as a function of frequency at −10 °C: ×, pure ice; O, 10^{-4} M NaCl ice; □, 10^{-3} M NaCl ice.

contaminated with 1.4×10^{-4} M HF. Measurements of bulk resistive currents as a function of temperature at 10 Hz gave linear Arrhenius plots with an activation energy of 0.3 eV for pure ice while 10^{-4} and 10^{-3} M NaCl had 0.18 and 0.16 eV, respectively, in agreement with published[1] values.

The addition of these impurities increased the resistive surface currents more than the capacitative ones. These currents could not be described by a Cole–Cole plot, but the currents below 2 kHz were roughly proportional with a phase angle of 14° for 10^{-4} M NaCl and 3° for 10^{-3} M NaCl. In Figure 7 the variation of the real surface conductivity of the doped ice over the range 0.1 to 30 kHz is compared with the behavior of pure ice. Over the complete range of frequencies the response of the doped ice can be described by a power law, both doping levels giving similar gradients of 0.2 and 0.18 for 10^{-4} and 10^{-3} M NaCl, respectively. The gradient in Figure 5 for pure ice is much greater, but only extends over a limited frequency range, with the low-frequency surface conductivity varying little

(6) Long, A. R. *Adv. Phys.* **1982**, *31*, 553–637.
(7) Maeno, M.; Nishimura, H. *J. Glaciol.* **1978**, *21*, 193–203.

with frequency. As a consequence, at 10 Hz the surface conductivity of the 10^{-4} M NaCl doped ice is six times greater than that of pure ice, but at 30 kHz the difference is only 20%.

When a contaminated sample was rimed with the same solution the effect was smaller than for pure ice, with the dc surface conductivity being reduced by only a factor of two. Similarly, rubbing the surface only decreased the surface conductivity by half. The surface conductivity of contaminated samples could also be reduced by growing frost on them. In all cases modifying the surface had no effect on the bulk currents.

Discussion

The measurements of the bulk conductivity of the samples of pure polycrystalline ice are in agreement with published values, fit well on a Cole–Cole plot, and can be explained in terms of a single Debye dispersion frequency.[1,5] From Figures 2–4 we can see that data for the surface conductivity cannot be fitted to a simple Debye model. Figure 4 shows that the increase in the real part of the surface conductivity starts at a lower frequency and that the increase extends over a much broader frequency range than the bulk, but an interpretation in terms of a spread of relaxation frequencies of the water dipole does not seem satisfactory. First such a spread should lead to a more elliptic Cole–Cole plot with its major axis closer to the ϵ' axis,[5] whereas Figure 3 shows that the reverse is true, and, second, one would expect that on the ice surface the dipole restoring force would be less and the dispersion frequency would be higher.

In any electrode arrangement the surface electrode will always detect some of the currents flowing in the bulk, and the test with conductivity paper modeling the electrodes used for this work indicates that there will be a small contribution. Generally this is unimportant, because the current detected by the surface electrode is much larger than the total current flowing to the bulk electrode, but near the dispersion frequency the imaginary component of the bulk current becomes large and could make a significant contribution to the signal sensed by the surface electrode.

The results of modifying the surface by frost, annealing, riming, and scratching lend further support to these ideas. These alterations had no effect on the bulk currents but resulted in dramatic changes in the real currents sensed by the surface electrode. However, changes in the imaginary currents were much less, and only about one quarter of the real ones. This would be consistent with a model in which three quarters of the imaginary currents sensed by the surface electrode was in fact flowing in the bulk. If this correction is made, then the surface current is even more resistive than indicated in Figure 3, and the Cole–Cole plot should be much closer to the vertical ϵ'' axis with a phase angle of less than 10°. We can be reasonably certain that the surface current is not totally real, because plots of the imaginary currents sensed by the two electrodes as a function of frequency are not identical in shape. The real and imaginary currents are related by the Kramers–Kronig transforms,[5] but because of the uncertainty regarding the exact magnitude of the surface currents the integrals are subject to error and so an independent check is not possible.

The high surface conductivity of ice is only one of the anomalous surface properties of ice. Fletcher[8] has proposed a semiquantitative model predicting the existence of a noncrystalline layer at the ice surface. Because the water molecules in ice have a finite electrical quadrupole moment, their electrostatic energy is lowered if they align, but there is an entropy penalty, so the Gibbs free energy is minimized at the surface if a noncrystalline disordered layer forms with some degree of dipole orientation. This model also predicts that there would be a high concentration of free ions on the surface which would account for the enhanced dc surface conductivity.

If this noncrystalline layer is responsible for the surface conductivity, it is not surprising that the simple Debye theory for a single dispersion does not apply. The behavior of the real surface conductivity with frequency for various temperatures is shown in Figure 5 and has a striking similarity to the published results for sputtered amorphous silicon (ref 6, p 607), in that the conductivity is fairly constant at low frequencies, but then follows a power law behavior at higher frequencies, and that a higher temperatures the transition to power law behavior occurs at higher frequencies. The data for films of amorphous arsenic tritelluride[9] and amorphous germanium[10] are also of similar form. If we follow the convention[6,11] used for amorphous materials and express the conductivity as

$$\sigma \propto \omega^s$$

then from Figure 5 the value of s for pure ice at −15 °C is about 0.65. In his review, Long[6] shows that the variation of s with temperature for amorphous semiconductors can give information concerning the electron conduction mechanism: tunneling should give a temperature independent s, correlated barrier hopping a value of s which falls with temperature, and polaron tunneling a value which increases with temperature. The lifetime of electrons[12] in bulk ice at −7 °C is only about 0.1 ns, so it seems improbable that they are the carriers on the ice surface. If the carriers on the ice surface are the protons predicted by Fletcher, then tunneling is unlikely; the hopping mechanism would predict a value of s which falls with rising temperature, in qualitative agreement with the ice behavior in Figure 5.

The models of Long's review assume that loss occurs by relaxation and that the varying environments surrounding the relaxing states lead to a broad distribution of relaxation times. An alternative viewpoint is described in a review by Hill and Jonscher[13] who invoke cooperative phenomenon. Jonscher[14] suggests that the value of the exponent s is related to the charge transport mechanism, but unfortunately unique predictions cannot be made. However, values of s close to unity seem to be associated with "intrinsic" processes and lower values with "extrinsic" processes due to some impurities or injected carriers. Thus it seems that the exponent 0.2 found in this work for NaCl-doped ice could arise from Na^+ or Cl^- ions on the surface, whereas the value of 0.65 for pure ice may be due to the free hydrogen ions predicted by Fletcher.

When the surface is altered and the surface disorder increased the dc surface conductivity appears to go through a maximum. At −10 °C single crystals have a dc conductivity of about 10^{-10} mho, and this increases if it is scratched with emery paper or a needle.[7] Polycrystals have a conductivity of about 5×10^{-9} mho and the results in this paper show that it is reduced if it is rubbed or small water

(8) Fletcher, N. H. *Phil. Mag.* **1968**, *18*, 1287–91.

(9) Rockstad, H. K. *J. Non-Cryst. Solids* **1970**, *2*, 192.

(10) Long, A. R.; Balkan, N.; Hogg, W. R.; Ferrier, R. P. *Phil. Mag. B* **1982**, *45*, 497.

(11) Mott, N. F.; Davis, E. A. "Electronic Processes in Non-crystalline Materials"; Clarendon Press: Oxford, 1971.

(12) Kunst, M.; Warman, J. M. *Nature (London)* **1980**, *288*, 465–7.

(13) Hill, R. M.; Jonscher, A. K. *Contemp. Phys.* **1983**, *24*, 75–110.

(14) Jonscher, A. K. *Nature (London)* **1977**, *267*, 673–9.

droplets are rapidly frozen on the surface; both these processes are known to produce defects in the ice. In contrast annealing the ice should lessen the disorder, and this did produce a rise in the conductivity. The effect of these changes on the ac conductivity was comparatively small.

These results can be explained qualitatively in terms of a simple model in which the current carriers are scattered many times per oscillation but can be trapped by defects or dislocations, leading to a well-defined mobility. As the frequency increases the amplitude of the oscillation will fall and the carriers are less likely to be trapped, leading to a higher mobility and the observed increase of conductivity with frequency. For dc conductivity the mobility will be controlled by the most difficult "hop" the carrier has to make and this could due to defects or dislocations. The conductivity is the product of the mobility and the carrier concentration. If the surface disorder is artificially increased, then according to Fletcher's theory, because the entropy penalty is less, it should become energetically favorable for more dipoles to align at the surface and thus the carrier concentration would increase. One can speculate that as the disorder of the ice surface increases the conductivity initially increases as the carrier concentration rises, but the conductivity subsequently falls as the mobility becomes the controlling factor. The variation of surface conductivity from one sample to another probably arises through different crystal size and structure. The conductivity of frost was low, possibly due the large number of grain boundaries between the many small crystals. Some support to these ideas on surface disorder is given by measurements of changes in contact potential during riming and rubbing.[15]

Conclusion

The results on the frequency dependence of the surface currents in polycrystalline ice indicate that the conduction mechanism is quite different from that of the bulk. There are similarities to the behavior observed in amorphous semiconductors, and this gives additional support to Fletcher's model which predicts a disordered noncrystalline layer on the surface of the ice. Experiments on the Hall effect and of doping with NH_3 and HF could give further information on the conduction mechanism.

If the inductive theory of thunderstorm electrification is to operate, it is important that the polarization charges induced by the external field are able to flow on to the smaller ice particle during the limited time available. Gaskell[2] has shown that the time constant involved is inversely proportional to the surface conductivity. Gaskell used the dc value, but the large ac values obtained in this work should be more appropriate. If we consider at 100-μm-diameter ice sphere approaching a larger target, then significant flow of the polarization charge on the target will only occur when the ice sphere is within two diameters of the target. For a velocity of 10 m s^{-1} this time will be about 20 μs. The high-frequency ac conductivity data obtained in this paper suggest an appropriate surface conductivity for pure and 10^{-4} M NaCl ice of about 1.5×10^{-7} mho, whereas for 10^{-3} M NaCl the value should be closer to 5×10^{-7} mho.

Laboratory experiments[4] using spherical 100-μm polycrystalline ice particles colliding with ice targets at 10 m s^{-1} in an electric field have shown that at −10 °C the inductive mechanism is not obeyed for pure or 10^{-4} M NaCl ice, but operates well for the more highly conducting 10^{-3} M NaCl ice. In the atmosphere the small ice particles are probably single crystals having even lower conductivities than in these experiments, and so we conclude that, in spite of the higher ac conductivities reported in this paper, it is likely that the inductive mechanism does not operate in the atmosphere.

Acknowledgment. This work was performed with the help of a scholarship from the CONICET, Buenos Aires, Argentina, and further financial support from Grant AFOSR 81-0189.

Registry No. Water, 7732-18-5.

(15) Caranti, J. M.; Illingworth, A. J. *J. Phys. Chem.*, this issue.

JOURNAL OF GEOPHYSICAL RESEARCH, VOL. 88, NO. C13, PAGES 8483-8489, OCTOBER 20, 1983

TRANSIENT WORKMAN-REYNOLDS FREEZING POTENTIALS

J. M. Caranti[1] and A. J. Illingworth

Pure and Applied Physics Department, University of Manchester Institute of Science and Technology

Abstract. There are two processes by which Workman-Reynolds freezing potentials may result in thunderstorm electrification or aircraft precipitation static. One possibility is that charge is transferred when supercooled drops splash on the hailstone or aircraft surface. Alternatively, freezing potentials may develop when cloud droplets freeze on these surfaces and persist long enough to affect charge transfer when ice crystals subsequently collide with the ice-covered surface. Laboratory experiments on the development of these freezing potentials when bulk supercooled solutions freeze, and when raindrops and cloud droplets freeze on impact with an ice surface, show that (1) any potentials developed are very much smaller than the published values for the quasi-static case; (2) in situations of atmospheric importance the drops will be supercooled, and such solutions are very much less efficient in developing potentials than non-supercooled ones; (3) cloud droplets freeze very rapidly, and if any freezing potential develops during this time, then it decays in less than 5 ms and is statistically unlikely to affect charge transfer in subsequent collisions with ice crystals. We conclude that in the atmosphere Workman-Reynolds potentials do not influence the charge transferred by colliding precipitation particles and briefly consider other relevant mechanisms.

1. Introduction

Large potential differences develop at the ice-water interface when dilute ionic solutions freeze, and it has been suggested that they play a role in thunderstorm electrification. They could also affect the static charging of aircraft flying through clouds containing supercooled water and ice. Following the original measurement of Workman and Reynolds (1949, 1950), other workers (Gross, 1965, 1982; Lefebre, 1967; Cobb and Gross, 1969) have confirmed that the potentials result from the selective incorporation of ions by the growing ice. For example, a solution of 10^{-4} M NaCl produced 30 V, the water being positive with respect to the ice, and the largest potential of 230 V was for a solution of 5 10^{-5} M ammonia with the ice positive.

Workman and Reynolds (1950) originally envisaged charging occurring as water was shed by graupel particles in wet growth. In view of the enormous potentials developed, the water shed should carry substantial charge. For most common contaminants including NaCl, the water lost would be positive and the graupel negative, and subsequent gravitational separation would lead to the observed structure of thunderstorms. Later, when it became clear that water was rarely shed from a growing hailstone but was retained in a spongy ice structure, Workman (1967) proposed that electrification resulted from the collision of hailstones with supercooled water drops several millimeters in diameter, which would be of sufficient size to splash off during impact.

Charge transfer associated with the splashing of raindrops on to hailstones has been studied in the laboratory by Workman (1967), Shewchuck and Iribarne (1971), and Bodhaine (1972); in these studies, drops of a few millimeters diameter at a temperature below 0°C collided with colder ice surfaces, and values of charge transfer per collision (pc) were around 10 pc. Shewchuck and Iribarne (1971) calculated that a sufficient number of these interactions could occur to give appreciable charging in mature thunderstorms. However, when these experiments were repeated by Latham and Warwicker (1980) with the drops supercooled to the ambient air and ice temperature as would occur in natural clouds, then the charge transfer was reduced by 3 orders of magnitude. They concluded that the charging resulted from disruption at the water-air interface rather than from freezing potentials and that it would be of negligible importance in cloud electrification.

Recent opinion has favored collisions between ice crystals and riming hailstones as the cause of thunderstorm electrification. Laboratory experiments simulating such collisions have measured charge transfers of the appropriate magnitude, and although the exact mechanism is unclear, when consideration is given to the capacitance at separation of the ice particles, potential differences of several hundred millivolts seem to be required. Differences in work function (or contact potential) of this magnitude between the interacting ice particles have been suggested as the driving force (Buser and Aufdermauer, 1977; Caranti and Illingworth, 1980; Gaskell and Illingworth, 1980).

This paper examines the possibility that the Workman-Reynolds freezing potentials may have an appreciable decay time so that after a supercooled liquid drop has frozen on the hailstone surface a potential of several hundred millivolts persists and results in the observed charge transfer during subsequent collision of ice crystals with the hailstone. If this occurs, then it could explain why charge transfer during ice crystal collisions is affected by contaminants in the ice as was reported by Reynolds et al.

[1]Permanently affiliated with IMAF, Cordoba, Argentina.

Paper number 3C0940.
0148-0227/83/003C-0940$05.00

(1957) and Jayaratne et al. (1983). Raindrops take several seconds to freeze, but a cloud droplet will be completely frozen after only a few milliseconds (Macklin and Payne, 1968), but in view of the rarity of raindrop collisions compared to the continual riming by supercooled cloud droplets, an ice crystal is more likely to collide with the hailstone surface formed from a recently frozen cloud droplet.

When a supercooled drop lands on an ice substrate, it freezes in two stages. In the first stage, dendrites propagate through the supercooled liquid, and Hallett (1964) reports propagation speeds at -10°C of 5 cm s^{-1}; then, during the second stage a well-defined front moves in the direction of the temperature gradient which should progress at about 1.5 cm s^{-1}; after 5 μm have been frozen (Macklin and Payne, 1967).

In measurements of freezing potential where the water is not supercooled, the first stage of freezing will be absent. The freezing potentials arise as a dynamic equilibrium between the rate of incorporation of ions in the advancing front and the relaxation of the charge due to the finite conductivity of the ice. Consequently, potentials do not develop when the freezing speed is less than 1 μm s^{-1} because the generation term is too low, and they generally peak for concentrations in the range 10^{-4} to 10^{-3} M, the conductivity term dominating for higher levels. In order to understand the phenomenon, most work has concentrated on the quasi-static measurements with freezing speeds too low to be of significance in cloud physics. For example, in the very detailed study of Cobb and Gross (1969) the freezing rates were in the range 10 to 1000 μm s^{-1}, and volumes of 35 ml were used, but a 10 μm droplet has only 10^{-10} of this volume and impacting on an ice surface at -10°C would freeze in about 10 ms. LeFebre (1967) developed an elegant theory, predicting that as a plane ice front advanced past a probe the freezing potential would rise for a few seconds and then fall, and this agreed with his observations. A different approach was used by Workman (1967) who measured the potentials developed when a copper rod at -15° or -20°C covered with 1-2 mm of ice was dipped into a cell containing water with various contaminants at 0°C. Although the water is still not supercooled, this method has the advantage that the initial freezing rate will be very high. He presents oscillograms that show potentials of up to several volts "for a minimum period of 30 to hundreds of milliseconds after contact". Except for $(NH_4)_2 CO_3$, the ice acquired a negative potential which then returned to zero within a second or so; it is not clear from the text whether this return is a real effect or due to the probe being removed from the water after its "brief contact". Varying contact potentials and blocking charges at the copper ice interface could have affected these results (Hobbs, 1974, p. 170).

The only measurements of Workman-Reynolds potentials developed by the freezing of supercooled solutions appear to be those of Pruppacher et al. (1968). Using temperatures between -2 and -11°C and initiating freezing by quickly lowering the temperature at one end of the polyethylene tube containing 2.1 cm^3 of solution, they detected a transient Workman-Reynolds potential during dendrite propagation which had the same sign and a maximum for the same concentration as the quasi-static case. A sharp peak in the potential was found about 1 s after freezing started, which then decayed to a relatively stable value until the dendrites reached the other end of the tube some 15 s later when a sharp peak in the opposite direction occurred.

Two questions are therefore unanswered. First, can freezing potentials develop during the short time while a small droplet is rapidly freezing on the surface of a hailstone? Second, if such potentials do develop, could the decay be slow enough so that a crystal in a cloud would have a reasonable probability of hitting the frozen droplet while the potential persisted?

When an ice surface is rimed with supercooled water droplets, the contact potential of the ice becomes more negative, the change in potential increases with greater supercooling reaching -500 mV at 15°C (Caranti and Illingworth, 1980, 1983). These riming contact potentials persist for many hours and are not affected by contaminants, and thus they are not a result of the Workman-Reynolds effect. The phenomena we are examining is a transient occurring during and perhaps shortly after freezing, after which a riming contact potential will remain, reflecting the temperature at which the rime was formed.

2. Experiments

The experiments can be divided into three categories. First, transient Workman-Reynolds potentials were measured for 20 ml samples of supercooled water. Second, these potentials were studied when rain size drops fell upon an ice substrate. Third, they were examined when small supercooled droplets landed on ice.

The freezing time scales in these three experiments are quite different. In the first case the complete freezing of the sample can take up to several hours depending upon the temperature, while in the second it takes only a few seconds and in the third a few milliseconds. Only the last of these three cases is of direct relevance to cloud physics. The freezing of raindrops on a hailstone is a rare event, and, of course, the freezing of 20 ml is out of the question, but, as we shall see, they contribute to our understanding of the phenomenon. Here, 10^{-4} M NaCl was generally used in the experiments because it is known to give a maximum Workman-Reynolds potential.

All previous measurements of freezing potentials have used two electrodes, one in the ice and one in the water. We have used a new approach and replaced the electrode in the water by a Kelvin vibrating capacitor, which, as it oscillated in the air just above the water surface, sensed the potential of the water with respect to the ice. An automatic phase-sensitive nulling circuit applied a backing-off potential to the vibrating capacitor so that no current flowed on or off it. This backing-off potential was equal to the potential of the surface of the water, and any rapid changes or transients in it

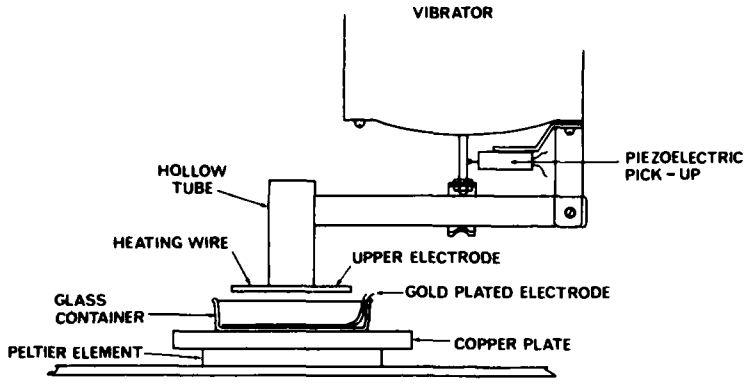

Fig. 1. Apparatus to measure potentials developed during the freezing of 20 ml of aqueous solution.

were recorded on a digital oscilloscope. Rapid response was achieved by using an electrode which vibrated at 500 Hz; the charge flowing to the capacitor during each half cycle was integrated, and the backing-off potential was adjusted to minimise the integrator output. Only a few cycles were needed to reach equilibrium, and so the time response was only 5 ms. This new method has several advantages. The presence of the electrode in the water would affect the heat flow during the freezing of small drops, and it could also give rise to varying contact potentials. By using the nulling method, negligible currents flow in the ice, thus minimizing any spurious potentials or blocking charges which could develop at the ice-metal surface. The potentials could be measured to better than 20 mV.

2.1. Freezing of 20 ml of Supercooled Aqueous Solution

As is shown in Figure 1, the solution was placed in a glass container 50 mm diameter and 12 mm deep, at the bottom of which was a gold-plated disc electrode connected to the exterior via an insulated wire. The temperature of the container was adjusted by placing it on top of a massive copper plate. The plate temperature was automatically controlled with a Peltier element.

The water was cooled slowly, and then, when at the required temperature, the freezing was initiated by touching it with a piece of ice. The temperature rose sharply as the dendrites propagated downward from the surface of the supercooled water, but, as maximum current automatically flowed through the Peltier element, the copper plate remained at a temperature only slightly higher than before freezing started. Consequently, both kinds of freezing occurred, first the dendrites filled the water with spongy ice, followed by a plane front growing from the electrode at the bottom of the container that eventually froze all the water.

Figures 2 and 3 display typical results showing that the potential had a peak similar in magnitude to those reported by Pruppacher et al. (1968). The major difference is that the reverse peak which they associated with the dendrites reaching the second electrode could not be detected. In these experiments the second electrode is not in the water. Figure 2 shows that for distilled water the water became negatively charged, while in Figure 3 we see that for 10^{-4} M NaCl the water was positively charged and the peak potential increased with greater supercooling. The rise time of about 1 s in Figures 2 and 3 coincided with the onset of the first stage of freezing. After about 12 s the first stage of freezing had ceased, and Figure 2 shows that while the second stage was progressing the potential was about -100mV. When freezing was complete, riming contact potentials could be detected. For Figure 2 this took several minutes, after which a constant potential of -100 mV persisted for many hours. If the ice surface was melted and refrozen slowly, then this potential returned to zero. If the supercooled water was colder, then the remanent value was larger, and the sign of the final contact potential was always negative for all contaminants irrespective of the sign of the transient; this is in accordance with our knowledge of riming potentials (Caranti and Illingworth, 1980, 1983).

2.2. Freezing of Rain Size Drops on an Ice Substrate

The glass dish in Figure 1 was replaced by a cylindrical polycrystalline ice sample of 50 mm diameter and 10 mm thickness, prepared by slowly freezing distilled water (10^{-6} mho cm^{-1}). The ice was heated with a hot air blower and the wet sample placed on the lower gold plated electrode

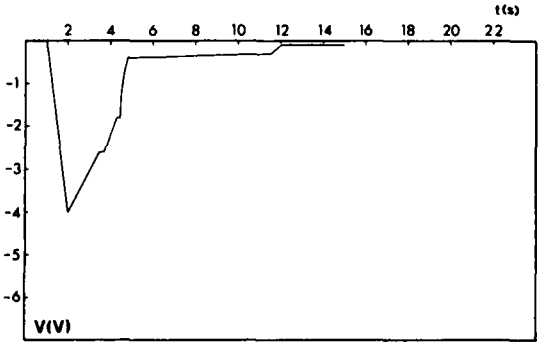

Fig. 2. Transient potential developed during the freezing of 20 ml supercooled water at -3°C. Liquid negative with respect to the ice.

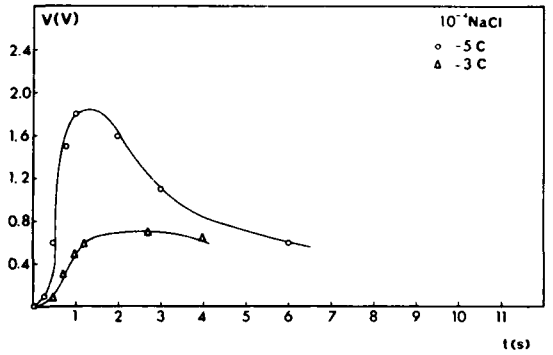

Fig. 3. Transient potential developed during the freezing of 20 ml of 10^{-4} M NaCl. Liquid positive with respect to the ice.

which was held just below 0°C. This method of sample preparation produced crystals of about 1 mm diameter with negligible stress and ensured good electrical contact. While monitoring the potential with the upper vibrating ring electrode, drops were allowed to fall down the axis of the ring on to the ice.

Figure 4 displays a typical result for three drops of 3 mm diameter of 10^{-4} M NaCl falling onto an ice surface at -20°C. In this case the drops were not supercooled but were near 0°C and impacted at 1.5 m s^{-1} which is much less than terminal velocity. The drops spread to a diameter of about 6 mm and so did not cover the ice surface; thus the actual freezing potentials were higher than in Figure 4 where the electrode was detecting an average potential of the unmodified ice and the potentials of the freezing drops. Figure 4 also shows that after reaching its maximum the freezing potential was linearly dependent upon the freezing speed derived from the theoretical treatment of Macklin and Payne (1967); in the absence of supercooling the first stage of freezing is absent, and, so, this unidimensional treatment is appropriate.

The reproducibility depended upon the drops spreading, but the general behavior was the same, with a rise time of about 0.6 s and a decay of 3 s. At higher ice temperatures, the potentials were smaller or even absent, at -10°C only occasionally exceeding 1 V. Experiments on a metal substrate yielded similar magnitudes, rise and fall times, and temperature dependence.

2.3. Transient Freezing Potentials During Riming

To study the development of freezing potentials as an ice surface was rimed, an arrangement was devised in which a cloud of 100 μm diameter supercooled droplets produced by an ultrasonic generator was allowed to impact on a moving ice surface. The principle is shown in Figure 5. The cloud was drawn past an ice-covered cylinder, and when this cylinder rotated, the droplets were carried under the vibrating electrode. Any Workman-Reynolds potential developed by the droplets when they were under the electrode could be detected. By varying the rotation speed any delay between landing and measurement could in principle be achieved. Therefore, by increasing the speed continuously from very low values, there should be a moment at which the system starts picking up any Workman-Reynolds potential superimposed on the normal riming potential.

The rotating cylinder was made out of copper tube which was electroplated with nickel. Its speed was monitored by using a toothed disc which chopped an infrared beam, and its temperature was measured by using a thermistor mounted inside the cylinder connected to the exterior

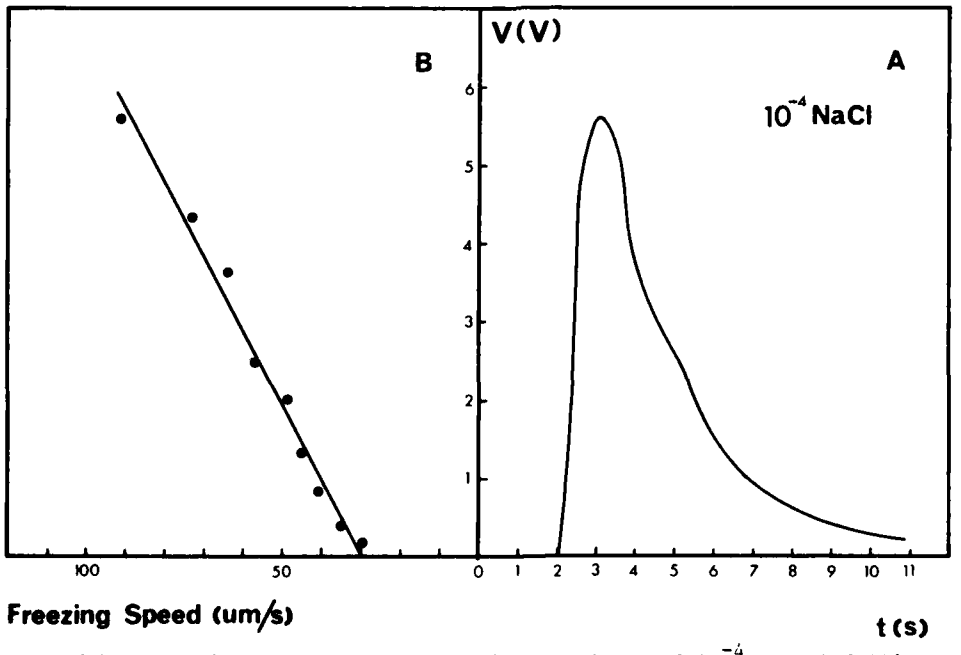

Fig. 4. (a) Potential developed by 3 mm diameter drops of 10^{-4} M NaCl falling on an ice surface at -20°C. Liquid positive with respect to the ice. (b) Potentials versus freezing speed calculated from Macklin and Payne [1967].

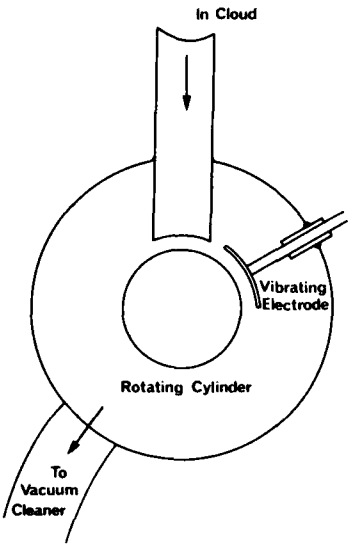

Fig. 5. Rotating cylinder apparatus to measure transient potentials developed during the freezing of 100 μm supercooled droplets.

via slip rings. The vibrating electrode was cylindrically shaped and built out of brass mesh electroplated with nickel. The electrode was split into two halves, one half measuring the potential of part of the rotating cylinder which was not exposed to the cloud. This served as a reference to compare with the potential of the part of the cylinder which was rimed and detected by the other half of the electrode. To prevent frost formation, both halves of the electrode were held at a temperature a couple of degrees above the ambient air temperature. This was achieved by using a thermistor mounted on the electrode to control the current through heating resistors.

Experiments were carried out over the temperature range -1°C to -20°C, using supercooled drops of distilled water, 10^{-3} M and 10^{-4} M NaCl, but no transient freezing potentials could be detected, although the sensitivity of the apparatus was better than 100 mV. As soon as the cylinder was completely covered with rime, the potential became constant and independent of the cylinder speed. A maximum liquid water content of 10 g m^{-3} was used which rimed about 10% of the ice surface per revolution.

The only potentials which were observed were those associated with the change in contact potential when an unrimed surface was rimed. If the rime was melted and then allowed to refreeze slowly, then this contact potential returned to its previous value. These riming potentials were very conspicuous when only half of the stationary cylinder was rimed, because on subsequent rotation of the cylinder the output oscillated between the two levels corresponding to the two kinds of ice.

Macklin and Payne (1967) have theoretically calculated that the freezing time of a layer of water is proportional to the square of its thickness, and the inverse of the supercooling of the substrate. We shall use their results and assume that the 100 μm droplets used in this experiment spread by a factor of 2 and are thus equivalent to a 20 μm thick layer. The first stage of freezing which involves the propagation of dendrites takes about 75 μs for a 15 μm layer at -20°C and 500 μs at -10°C and therefore cannot be detected with this apparatus. However, the second stage for a 20 μm layer at -10°C takes 24 ms to complete; the times at -1°C and -20°C being 240 and 12 ms. These times should be easily resolved as the speed of the cylinder is increased to its maximum value which corresponds to a delay of only 5 ms between riming and detection.

3. Discussion

The Workman-Reynolds potentials developed when 20 ml of supercooled distilled water or 10^{-4} M NaCl were frozen showed a sharp initial peak with a rise time of about a second which coincided with the first stage of freezing, but while the second stage was progressing it decayed to very small values. The secondary peak, intercepted by Pruppacher et al. (1968) as the arrival of the dendrites at the second electrode was not observed in these studies, which seems reasonable as the second electrode was not immersed in the liquid. In this work the first peak occurred as the dendrites propagated down from the surface before reaching the electrode. The size of the first peak appeared to increase with the degree of supercooling, as would be expected if the potential results from a balance between charge generation and loss. The absence of potential during the second stage of freezing as the plane front moves slowly through the dendrite network implies that the cellular structure of the spongy mixture of water and ice hinders the orderly charge separation. As a consequence, the charge generated in the first stage leaks away, but no further separation in any preferred direction can take place and only a small potential is generated.

The results with the drops of 10^{-4} M NaCl landing on an ice substrate support the idea that nonsupercooled drops are more efficient at separating charge than supercooled ones. If the ratio of the areas of the electrodes and the droplets is taken into account, then the potential developed by the 3 mm diameter nonsupercooled drops is at least an order of magnitude larger than for the 100 μm supercooled droplets. Calculations show that the freezing time of the 3 mm drops was about 50 s, but the potentials had decayed after about 3 s, so it seems that as soon as the freezing speed decreased the generation slowed down. For the 100 μm droplets the first stage of freezing should take 75 μs and the second stage 10-24 ms; no potentials could be detected, either because the droplet volume was so small that the total charge separated lead to an insignificant potential or that the potential had already decayed in the 5 ms minimum response time of the apparatus.

We can now resolve some of the disagreements of previous work referred to in the introduction. If the dendrite network hinders orderly charge separation, then this explains why Latham and Warwicker measured charge transfers when raindrop-sized drops collided with ice targets which

were 3 orders of magnitude less than previous workers who had not correctly supercooled their drops. Furthermore, the freezing potentials which were detected in this work had rise times of about 1 s and thus should be of negligible value during the interaction of a hailstone with a raindrop which lasts only for a few milliseconds. Workman (1967) recorded large potentials with a very rapid rise time when he dipped an ice-covered probe into nonsupercooled water. In this case the first stage of freezing will be absent and the dendrite network will not exercise its inhibitory influence. Although of interest in explaining the development of Workman-Reynolds potentials, it is difficult to see how experiments with nonsupercooled drops can be of direct relevance to the problem of charge separation in the atmosphere. The equations describing the movement of ions by electrical and diffusion forces referred to a frame that moves with the front are given by Pohl (1954) and have been solved for a steady state freezing rate by Warwicker (1978). However, extending these calculations to a variable freezing rate appears difficult and seems intractable in a situation where there is a dendrite network.

4. Conclusion

The experimental evidence indicates that negligible charge separation occurs during the interaction of hailstones with supercooled raindrops and that if any Workman-Reynolds potentials are developed during riming of hailstones they should have no influence on charge transfer in subsequent collisions of the hailstone with ice crystals. In a recent paper, Gross (1982) has pointed out that Hertzian theory predicts that the contact time for collisions of ice crystals with hailstones should be less than a microsecond, and because the electrical relaxation time derived from the bulk conductivity is a few milliseconds charge flow should be negligible, unless the ice surface is wet, or the charge carriers are electrons which can tunnel in the short time available between surface states in the two ice particles. He concludes that in these two cases the charge transfer must be driven by the interphase field or the temperature field, respectively.

As was already observed, the interactions leading to the shedding of water from wet hailstones are infrequent and the charge transfer per event too low. Gross (1982) assumed that the relaxation time for charge flow in ice-ice collisions is governed by the bulk conductivity, but it is well known that the conductivity of single crystals of pure ice smaller than a few millimeters is dominated by the surface (Hobbs, 1974). In an independent analysis of the same problem, Gaskell (1981) has calculated τ_s, the time for the redistribution of charge carriers across the surface conducting layer which is given by $\tau_s = d\ \varepsilon\ \varepsilon_o/\lambda_s$ where d is its thickness, ε the relative permittivity, and λ_s the surface conductivity. Gaskell took the thickness to be that of the disordered "liquid-like" layer estimated by Fletcher (1968) to be 2 nm, and, using $\lambda_s = 10^{-10}$ mho and $\varepsilon = 100$, deduced that τ_s was about 20 ns. Direct measurements using proton channeling (Golecki and Jaccard, 1977) have yielded a value of d about 20 times larger; however, the value of λ_s for polycrystalline ice on the surface of a hailstone is probably nearer to 10^{-8} mho (Camp et al., 1969).

It thus appears that during a collision between ice particles there is sufficient time for the charge carriers present in the surface conducting layers to transfer across the area of contact. These carriers could be ions as predicted by Fletcher. Although surface states may be involved they need not be invoked. Lowell and Rose-Innes (1980) have suggested that intrinsic surface states can occur in covalent solids, but for molecular ones like ice they are quite unlikely to exist or, if they do, they will be very near to the band gap border.

The thermoelectric effect favored by Gross (1982) as the ice-ice charge transfer mechanism has two major drawbacks. First, the potentials are too small, being only about 2 mV^oC^{-1} and, second, they take about 10 ms to develop and, so, during the microsecond collision time would be quite negligible. Differences in contact potential of several hundred millivolts remain as a possible explanation for the charge transfer during ice-crystal hailstone collisions.

It appears that Workman-Reynolds potentials should not affect aircraft precipitation static, because although supercooled droplets can splash off aircraft they should not separate any charge by this mechanism and because the freezing potentials decay so rapidly they should not influence the charge transferred when crystals collide with ice-covered wings. We are forced to conclude that although Workman-Reynolds potentials are initially attractive in view of their enormous magnitude in the quasi-static case, when consideration is given to the short contact times involved, they are not of importance in the atmosphere.

Acknowledgments. This work has been performed with support of the EOARD under grant AFOSR 81-0189. We would like to thank Peter Kelly for his assistance in the workshop.

References

Bodhaine, B. A., The effects of ammonia on the electrification of freezing and splashing water drops, Tellus, 24, 473-480, 1972.

Buser, O. and A. M. Aufdermauer, Electrification by collisions of ice particles on ice or metal targets, in Electrical Processes in Atmospheres Steinkopff. Darmstadt, 1977.

Camp, P. R., H. Kiszenick, and D. Arnold, Electrical conduction in ice, in Physics of Ice, Plenum, New York, 1969.

Caranti, J. M., and A. J. Illingworth, Surface potentials of ice and thunderstorm charge separation, Nature, 284, 44-46, 1980.

Caranti, J. M., and A. J. Illingworth, The contact potential of ice, J. Phys. Chem., in press, 1983.

Carras, J. N., and W. C. Macklin, The shedding of water during hailstone growth, Q. J. R. Meteorol. Soc., 99, 639-648, 1973.

Cobb, A. H., and G. W. Gross, Interfacial electric effects observed during the freezing of dilute electrolytes in water, J. Electrochem. Soc., 116, 796-804, 1969.

Fletcher, N. H., Surface structure of water and ice, II, A revised model, Phil. Mag., 18, 1287-1300, 1968.

Gaskell, W., A laboratory study of the inductive theory of thunderstorm electrification, Q. J. R. Meteorol. Soc., 107, 955-966, 1981.

Gaskell, W., and A. J. Illingworth, Charge transfer accompanying individual collisions between ice particle and its role in thunderstorm electrification, Q. J. R. Meteorol. Soc., 106, 841-854, 1980.

Golecki, I., and C. Jaccard, The surface of ice near 0°C studied by 100KeV proton channeling, Phys. Lett., 63A, 374-376, 1977.

Gross, G. W., The Workman-Reynolds effect and ionic transfer processes at the ice solution interface, J. Geophys. Res., 70, 2291-2300, 1965.

Gross, G. W., Role of relaxation and contact times in charge separation during collision of precipitation particles with ice targets. J. Geophys. Res., 87, 7170-7178, 1982.

Hallett, J., Experimental studies on the crystallization of supercooled water, J. Atmos. Sci., 21, 671-682, 1964.

Hobbs, P. V., Ice Physics, Clarendon, Oxford, 1974.

Jayaratne, E. R., C. P. R. Saunders, and J. Hallett, Laboratory measurements of electric charge transfer during multiple ice-ice collisions, Q. J. R. Meteorol. Soc., in press, 1983.

Latham, J., and R. Warwicker, Charge transfer accompanying the splashing of supercooled raindrops on hailstones, Q. J. R. Meteorol. Soc., 106, 559-568, 1980.

Lefebre, V., The freezing potential effect, J. Colloid Interface Sci., 25, 263-269, 1967.

Lowell, J., and A. C. Rose-Innes, Contact electrification, Rep. Prog. Phys., 29, 947-1023, 1980.

Macklin, W. C., and G. S. Payne, Theoretical study of the ice accretion process, Q. J. R. Meteorol. Soc., 93, 195-213, 1967.

Macklin, W. C., and G. S. Payne, Some aspects of the accretion process, Q. J. R. Meteorol. Soc., 94, 167-175, 1968.

Pohl, R. J., Solute redistribution and recrystallization, J. Appl. Phys., 25, 1170-1178, 1954.

Pruppacher, H. R., E. H. Steinberger, and T. L. Wang, On the electrical effects that accompany the spontaneous growth of ice in supercooled aqueous solutions, J. Geophys. Res., 73, 571-584, 1968.

Reynolds, S. E., M. Brook, and M. F. Gourley, Thunderstorm charge separation, J. Meteorol., 14, 426-436, 1957.

Shewchuk, S. R., and J. V. Iribarne, Charge separation during splashing of large drops on ice, Q. J. R. Meteorol. Soc., 97, 272-282, 1971.

Shewchuk, S. R., and J. V. Iribarne, Electrification associated with droplet accretion on ice, J. Atmos. Sci., 31, 776-786, 1974.

Warwicker, R., Electrification by splashing of supercooled raindrops on hailstones, Ph.D. Thesis, Univ. of Manchester, England, 1978.

Workman, E. J., The production of thunderstorm electricity, J. Franklin Inst., 283, 540-557, 1967.

Workman, E. J., and S. E. Reynolds, A suggested mechanism for the generation of thundercloud electricity, Phys. Rev., 74, 709, 1949.

Workman, E. J., and S. E. Reynolds, Electrical phenomena occurring during the freezing of dilute aqueous solutions and their possible relationship to thunderstorm electricity, Phys. Rev., 78, 254-259, 1950.

J. M. Caranti, IMAF, Lapida 854, 5000 Cordoba, Argentina.

A. J. Illingworth, Department of Physics, The University of Manchester Institute of Science and Technology, P.O. Box 88, Manchester M60 1QD, England.

(Received December 7, 1982;
revised May 23, 1983;
accepted May 31, 1983.)

To be presented at the Sixth International Atmospheric Electricity Conference 3-8 June 1984, SUNYA, Albany, New York, USA, and then submitted to the Journal of Geophysical Research for publication.

ICE CONDUCTIVITY RESTRAINTS ON THE INDUCTIVE THEORY OF THUNDERSTORM ELECTRIFICATION

A J Illingworth*, J M Caranti+

*Physics Department, UMIST
Manchester M60 1QD, ENGLAND

+IMAF, Cordoba 5000, ARGENTINA

1. INTRODUCTION

The inductive theory of thunderstorm electrification has been favoured by many recent workers (e.g. Mason 1972, Sartor 1981), who have concluded that it can account for the observed rapid growth of the electric field to produce lightning. According to this mechanism when a small cloud particle (radius r_a) bounces off the underside of a larger falling precipitation particle (radius r_b) in the presence of an external electric field (E), then the small particle will remove some of the charge (q) induced on the surface of the large particle by the external field, given by

$$q = (\pi^2/6)(r_a^2/r_b^2)(12\pi\epsilon_o r_b^2 E\cos\phi + Q_b) \qquad (1)$$

where Q_b is the initial charge on the large particle, $r_a \ll r_b$, and ϕ the angle between the direction of field and the radius to the point of contact. Gravitational separation of the two particles results in an enhancement of any pre-existing field, so that subsequent collisions separate more charge and an exponential growth of the field should follow. Because interactions involving liquid water usually result in coalescence, collisions between small ice crystals and larger hail or graupel particles have generally been the favoured candidates.

The mechanism is very attractive in view of its simplicity and the positive feedback which should result in rapid field growth, however, because of the finite conductivity of the ice it is not clear that the charges can flow during the short interaction time available. Gross (1982) pointed out that the relaxation time derived from the bulk conductivity of ice was much greater than the submicrosecond contact times calculated from Hertzian collision theory, and deduced that the inductive mechanism should not operate. In an independent analysis of the same problem, Gaskell (1981) showed that for particles of the size found in the atmosphere the surface conductivity will dominate, and, using the single crystal DC data available, calculated electrical relaxation times of about 100μsec. As adhesive forces could lead to longer contact times than those predicted by the simple Hertzian theory, he was unable to reach a firm conclusion without resorting to experiment.

Laboratory studies of the effect of an external electric field on the charge transferred during collisions of small ice particles with larger ice targets have yielded conflicting results. Latham and Mason (1962), Aufdermauer and Johnson (1972), Buser and Aufdermauer (1977), Takahashi (1978) and Gaskell (1981) using small crystals or frozen water droplets of sizes 50μm, 100μm, 20μm, 10 to 100μm, and 100μm respectively, found either no field dependent charging or such a variability that the results were inconclusive. Scott and Levin (1970) showed that inductive ice-ice charging does occur for large 1mm natural ice crystals colliding with a 2.5cm ice coated sphere at $1ms^{-1}$, but these very long contact times are unlikely to occur in natural clouds.

In this paper we present the results of a laboratory study of the field dependence of the charge transfer during ice-ice collisions as a function of the surface conductivity of the ice. The results are interpreted in terms of recently available data on the AC surface conductivity of doped and pure ice (Caranti and Illingworth, 1983). In the inductive mechanism, the charges transferred are polarisation charges which flow along the surface of the ice and so will be affected by the finite surface conductivity. Gaskell (1981) pointed out that when two particles collide and charge is transferred across the interface where the contact occurs, then a different, negligibly short, time constant is applicable.

2. EXPERIMENTAL APPARATUS

The charge transferred when a single small ice particle collided with an ice covered target was measured by the apparatus shown in Fig. 1, which is broadly similar to that used in earlier studies by Gaskell and Illingworth (1980) and Gaskell (1981). Previously workers (e.g. Reynolds et al, 1957) have often measured the currents flowing to a target when a cloud of ice crystals flowed past, and calculations of the charge per interaction have depended upon uncertain and varying crystal concentrations and separation efficiencies.

Water droplets in the size range 50-200μm with a controllable charge (0 to ~ 50fC) were produced at the rate of about 1Hz by an Abbott and Cannon (1972) droplet generator on top of the cold room. Each droplet then froze slowly as it fell down a tube into the cold room and collided with a tenuous cloud of minute ice crystals, which was formed by cooling a short section of the tube. In the previous studies with this apparatus, the particles were frozen in an unrealistic manner by cooling to near liquid nitrogen temperatures. Such abrupt cooling also produced a very opaque ice cloud so that the ice particle acquired an unpredictable and varying charge as it collided with the dense cloud.

The time for the particle to pass between two induction rings placed just below the freezing section then enabled the terminal velocity of each particle to be determined, and hence the size estimated to better than 10um. After falling a further 60cm to reach thermal equilibrium, the small ice particle was accelerated in a wind tunnel (typically to $5ms^{-1}$) and then passed through another induction ring before hitting the target, which was an ice coated cylinder 4mm in diameter. When a voltage X was applied to the field rings above and below the target there was a uniform field of $220 X\ Vm^{-1}$ at the target surface; this factor was estimated from a model with conductivity paper. For a radial field configuration the factor 12π in equation (1) becomes 4π.

Separate amplifiers were placed as close as possible to both the induction ring and the target to reduce microphonic and 50Hz pick up to the equivalent of less than 2fC. The amplifier outputs were summed, recorded, and subsequently replayed and examined on a digital storage oscilloscope. Because the amplifier has a rise time of 50usecs but a long (100msec) decay time for any charge deposited on the target, it was possible to differentiate between the rapidly varying induced charges caused by approaching and departing charged particles, and the long 100msec exponential decay when charge was transferred to the target. Considerable information on the nature of the interaction could be derived from the shapes of the waveforms as shown in Figure 2. In all cases the first pulse is the passage of the particle through the induction ring with its initial label charge, q_i. The start of the second excursion of each waveform is the charge induced on the target as the particle approaches, and from the elapsed time since the passage through the induction ring the velocity of impact may be calculated. Subsequently, on actual collision a variety of waveforms are possible transferring charge q_t to the target as shown in Figure 2 and described below:

a) If the second pulse is smaller than the first, then the particle has just missed the target, such waveforms are of great help when trying to align the apparatus. When the two pulses are equal there is an ambiguity; either the particle has passed very close to the target but just missed it, or it has collided and separated but no charge has been transferred.

b) Either the particle has hit the target and stuck to it - a 'collection'; or it has collided, donated its charge to the target, and then left carrying no charge.

c) The particle has collided with and separated from the target, transferring to the target an amount of charge (q_t) equal to a fraction of the initial charge (q_i) on the particle.

d) Positive charge ($>q_i$) has been acquired by the target.

e) Negative charge has been acquired by the target.

f) As for d), but after collision the ice particle has rebounded upstream and then been accelerated and passed close to the target within 'electrostatic range' inducing the blip superposed on the exponential decay.

g) An extreme case of f) in which the particle has rebounded upstream and then bounced a second time on the ice target and transferred additional charge during the second interaction.

h) Initially appears to be similar to a), but the presence of the third pulse confirms that the particle has bounced upstream and then passed close to the target; this cannot be a collection but must indicate an interaction with zero charge transfer.

In examples f), g) and h) the rebounding and subsequent sensing of the particle indicate a more head-on collision, whereas the earlier waveforms will tend to reflect a more equatorial or grazing interaction. There is an equivalent set of waveforms for negative initial label charge. On occasion more complex waveforms are observed which initially appear to violate charge conservation, until it is realised that the particle must have bounced from the target to the wall where it acquired a spurious charge before being sensed by the target amplifier a second time. Such pulses were rejected.

For the analysis to be reliable it is essential that the small ice particle carries a clearly recognisable initial label charge (q_i), so that genuine interactions can be identified by the regular succession of pulses of constant height detected by the induction ring. All other events, due to extraneous ice crystals or occasional specks of dust within the tube hitting the target, can result in large charge transfers and are thus rigorously excluded from the data set.

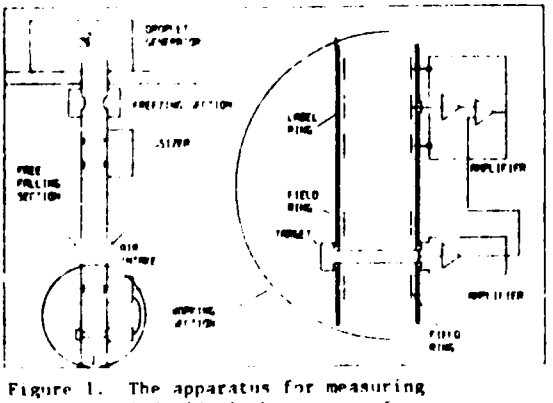

Figure 1. The apparatus for measuring individual charge transfers. Tube diameter 19mm.

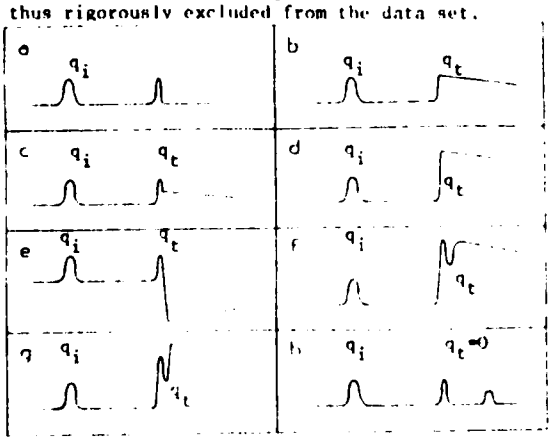

Figure 2. A selection of the various possible waveforms from the amplifiers. For explanation see the text.

3. RESULTS

3.1 Introduction

Unless stated to the contrary all the experiments described in this section were carried out at -10°C with 100μm diameter ice spheres colliding with the ice covered target at $5ms^{-1}$. These values were felt to reflect conditions within the cloud and also enabled comparisons with published data. As the field was radial, the cosϕ term in equation 1 was always unity, the constant was 4π, and since the amplifier held the target at virtual earth, Q_B was zero. The smooth ice target was prepared by dipping a gold-plated brass rod, which was just below 0°C, into the NaCℓ solution at 0°C. The conductivity of the solutions (10^{-2}M to 10^{-5}M) was continually monitored to check the concentration. In the majority of the experiments the same solution was used for the target and the frozen droplets. Although the interactions were apparently identical, each individual charge transfer was variable, and the data points displayed are all averages of at least 40 events.

As observed in the previous section, in order to identify genuine events, it was essential that the small particle carried a charge (q_i) before it hit the target. This presented some problems in the interpretation of the waveforms. If the two particles could be considered as good conductors for the time scales involved, then q_i should be rapidly donated to the target, to be followed by the field driven inductive transfer (q_E) given by equation 1. Consequently if q_t is the total charge acquired by the target then the field driven component of the charge transfer is equal to (q_t-q_i). However if the ice is acting as a poor conductor then none of the initial charge q_i will have time to 'leak' to the target, and the field dependent charge transfer q_E is simply q_t. For an intermediate case where the ice is partially conducting then a fraction (f) of the initial charge (q_i) 'leaks' to the target, and the field driven charge transfer is given by

$$q_E = (q_t - f.q_i) \qquad (2)$$

In the case of the non-conducting ice the term 'label' is appropriate because it plays no part in the charge transfer and can simply be considered as an identifier tag.

This method of analysis depends on knowing the factor f, which is itself an indicator of whether the inductive mechanism should be operating; for insulating ice (f=0) q_E should be zero, and for conducting ice (f=1) then q_E would be expected to obey equation 1. Consequently an initial series of experiments was carried out to ascertain the appropriate value of f. In the absence of an external field the fraction of the label which 'leaked' to the target was measured. Any non-field dependent charging mechanism would show up as an asymmetry of the leakage of labels having different polarity, but even this effect can be minimised by using large labels.

In the main sequence of charge transfer experiments in the presence of an external field, both polarities of label (q_i) were used so that the two values of q_E obtained from equation 2 could be compared for consistency. This agreement could then be contrasted with that found when extreme values of f=0 or 1 were substituted. As a final check for consistency, if f=1 the variation of q_E with field (E) should be that predicted by the inductive mechanism in equation 1, but for less conducting ice the charge transfer should be reduced by a factor f.

3.2 Leakage of the Initial Charge with no External Field

The waveform expected if half (f=0.5) of the initial charge on the small particle leaks to the target is shown in Figure 2c. Unfortunately the waveform for zero leakage (Figure 2a) is ambiguous as it can also result from a near miss, and zero leakage can only be confirmed if the small particle bounces and its subsequent promixity to the target is sensed as in Figure 2h. A similar problem arises for f=1 and complete leakage of the label occurs, because a simple collection of the particle by the target will yield the same waveform (Figure 2b). Consequently waveforms of the shape shown in Figures 2a and 2b, which may contain valid data, had to be excluded from the analysis, and so there is a tendency to underestimate f when it is near unity, and conversely to overestimate it when its true value is zero.

Table 1 summarises the results of the leakage experiment for both signs of label in the absence of an external field for various levels of doping of the ice. From these results it is clear that the 10^{-2}M NaCℓ ice is acting as a good conductor. Even though many interactions were rejected as possible collections the value of f is over 0.9. From previous studies it is known that a large proportion of small particles stick at -5°C but that the number at -10°C is low, and so a value of f=1 will be used in subsequent analysis.

Concentration	T	Q_i(FC)	Leakage	Q_i(FC)	Leakage	f
10^{-2}	-10°C	+30	90%	-30	96%	1.00
10^{-4}	-10°C	+ 8	35%	-10	25%	0.30
10^{-3}	-5°C	+18	87%	-13	82%	0.85
	-10°C	+24	55%	-10	66%	0.60
	-17°C	+16	29%	-16	28%	0.29
	-24°C	+24	15%	-14	18%	0.16
10^{-5}	-10°C	+19	-60%	-15	40%	

Table 1. Leakage of the initial charge in the absence of an external field. The factor f is used in Equation 2 in subsequent analysis.

The behaviour of the 10^{-4}M NaCℓ ice is quite different, and although there was considerable scatter in the individual leakages, a value of 0.3 for f was derived. We suspect that this value is rather high, as several waveforms with zero leakage (Figure 2a) had to be discarded; it appears that during these runs most collisions were predominantly grazing as few bouncing interactions of the form shown in Figure 2h were observed.

The results with the 10^{-2} and 10^{-4}M NaCl suggested that the 10^{-3}M should be an intermediate case, and so a series of runs at different temperatures was performed. As shown in Table 1 the value of f fell from 0.85 at -5°C to 0.16 at -24°C. The low values of f are, in this case, felt to be more reliable, because during this run bouncing collisions with zero charge transfer (Figure 2h) occurred quite frequently. As will be appreciated with this apparatus the position of impact of the

100μm particles on the target varies by a mm or so from day to day.

The results for the 10^{-5}M NaCℓ had quite a different character. In the absence of an electric field the charge transferred to the target was often negative and quite variable irrespective of the initial sign of the label. Consequently the concept of 'leakage' becomes rather meaningless. By comparison with the 10^{-4}M results we must assume that f=0, and that we are observing non field-dependent charging. This non-inductive ice-ice charging with the larger particle acquiring negative charge has, of course, been observed before, but its origin is at present obscure. As this non-inductive charging is not found for higher levels of doping, it appears that this mechanism is somehow neutralised or 'short circuited' by the more highly conducting ice.

3.3 Field-Dependent Charging

The field-dependent charge transfer for 10^{-2}M NaCl ice calculated using equation (2) with f=1 is plotted in Figure 3. Each point represents the average charge transfer for one value of label. Errors are typically ±4fC, but to avoid congestion are not drawn on the graph. The solid line is equation (1) and shows that with this highly conducting ice the inductive mechanism is being obeyed. This is consistent with the unity value of f derived previously. Several waveforms of the same shape as Figure 2g were observed, and interpreted as double bounces; in each case negligible charge was transferred on the second impact as would be expected if complete inductive charge transfer had occurred during the first impact. If the label, q_i, was not subtracted from the measured q_t, then the results were far less consistent. For example the two points at $-22.5 kVm^{-1}$, the q_E of -7fC was derived from an average q_t of -1fC with q_i +6fC; and the q_E of -12fC from q_t = -24fC and q_i = -12fC. The effect on the data for the $-67.5 kVm^{-1}$ field is more striking as summarised in Table 2.

q_E (fC)	q_t (fC)	q_i (fC)
-23	+10	+33
-24	-39	-15
-25	-37	-12

Table 2. The charges transferred to the target (q_t), the initial particle charges (q_i), and the calculated field driven charge transfer (q_E) for 100μm particles colliding with a target at -10°C at $5ms^{-1}$ in a field of $-67.5 kVm^{-1}$. Ice prepared from 10^{-2}M NaCℓ.

Far less field dependent charge transfer was observed when 10^{-4}M NaCℓ ice was used as shown in Figure 4, where the values have been calculated using f=0.3, and the solid line is 30% of the predicted inductive charge transfer. As indicated in Section 3.2 if a value of f=0.2 had been used the agreement would have been better. A series of experiments was carried out at the same temperature of -10°C, but with the size of the small particle increased to 150μm, and these should be compared with the dotted line which has a gradient 2.25 times greater than the 100μm line. Reasonable agreement is obtained, verifying the dependence on r_s^2 in equation (1). For all these interactions with 10^{-4}M NaCℓ ice,

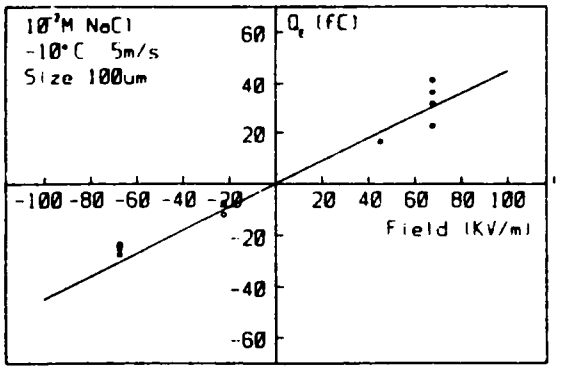

Figure 3. Field dependent charge transfer (q_t) for 10^{-2}M NaCℓ ice at $5ms^{-1}$ and 10°C. Diameter of the small ice sphere 100μm.

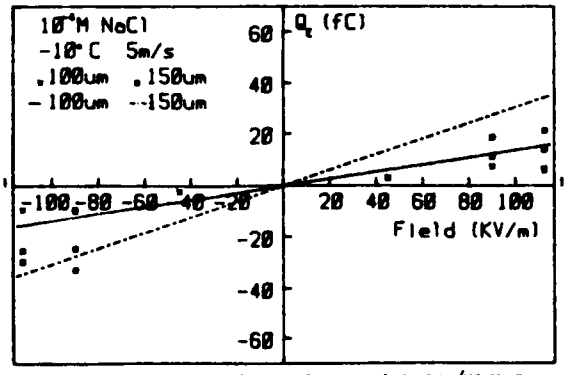

Figure 4. As for Figure 3 but with 10^{-4}M NaCℓ ice and two sizes of small ice particles.

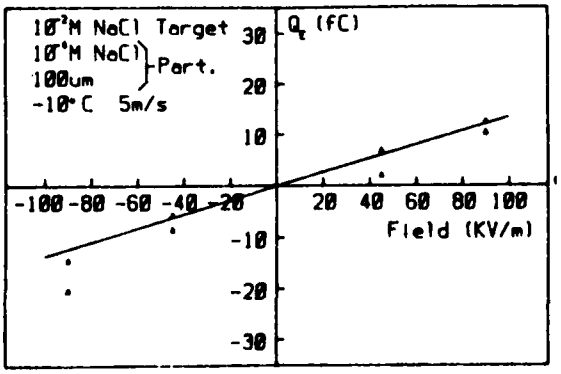

Figure 5. As for Figure 3 but the target of 10^{-2}M NaCℓ ice and the 100μm ice spheres of 10^{-4}M NaCℓ ice.

the scatter of the charge transfers was greater than with the 10^{-2}M ice, and the standard deviation for each point on Figure 4 is about ±7 fC.

Figure 5 demonstrates that when unequal doping was used, with a target of 10^{-2}M and 100um particles of 10^{-4}M NaCl ice, the results were not significantly different from those when both were of 10^{-4}M NaCl ice. This confirms that the polarisation charges have to migrate along both ice surfaces, and are limited by whichever movement is the most difficult. The situation is analagous to the total resistance of two unequal resistors in series.

The results of a series of runs carried out using 10^{-3}M NaCl for the same temperature range as the leakage measurements in Section 3.2 are displayed in Figure 6. The general trend is obvious, with the inductive mechanism being increasingly obeyed at the higher temperatures. The two straight lines represent 85% and 16% of the inductive mechanism. The individual transfers showed quite a scatter, and so the errors of the points are rather high. Although the results at -24°Cand -17°C do not appear to be very different, the average field-driven transfer was only ±5fC, and so any variation may have been obscured by amplifier noise which was equivalent to 2fC. The gradients for the -5°C and -10°C data are much steeper and are consistent with partial operation of the inductive mechanism.

Finally Figure 7 shows the results with the 10^{-5}M NaCl ice at -10°C. There is no tendency for field-dependent charging. This absence is not unexpected in view of the leakage results in Section 3.2. The individual charges showed a considerable scatter with occasional transfers of over -30fC for all values of the applied field.

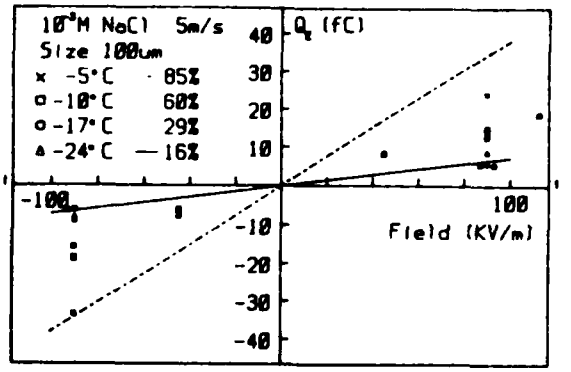

Figure 6. The field dependent transfer (q_E) for 10^{-3}M NaCl ice for various temperatures.

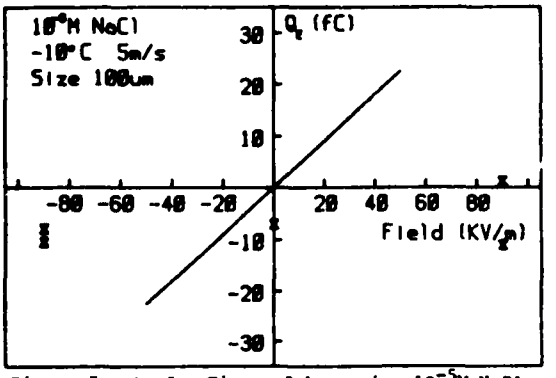

Figure 7. As for Figure 3 but using 10^{-5}M NaCl for the small particle and the target.

4. DISCUSSION

The pattern of the results is quite clear. As the conductivity of the ice increases, either due to more doping or a rise in the temperature, the inductive mechanism is increasingly well obeyed. We now discuss whether these changes are in agreement with our knowledge of the surface conductivity of doped ice, and then consider what levels of contaminants are appropriate for natural ice.

An Arrhenius plot of the surface conductivity of pure ice, 10^{-4}M NaCl, and 10^{-3}M NaCl ice at 10Hz as a function of temperature (taken from Caranti and Illingworth (1983)) is shown in Figure 8. Caranti and Illingworth also found that the conductivity increased with frequency, ω, as $\omega^{0.3}$, so that the ratio of the conductivities at 10^{-4} and 10^{-3}M NaCl remains the same at all frequencies, but at 30kHz the conductivities were about 5 times the value at 10Hz. Unfortunately no 10^{-2}M data is available, but from Figure 8 it is evident that the conductivity of the 10^{-4}M NaCl at -10°C is about the same as the 10^{-3}M ice at -24°C. An Arrhenius plot of the variation with temperature of the leakage fraction, f, for the 10^{-3}M NaCl ice is displayed in Figure 9. From this Figure an activation energy of 0.55eV can be derived, in good agreement with the energy of 0.5eV found from the 10^{-3}M slope in Figure 8. This shows that over this range of f, the leakage factor is proportional to the surface conductivity, and that the data on field-driven charge

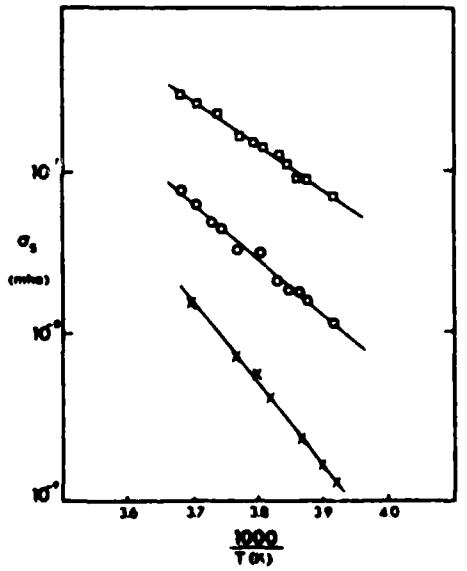

Figure 8. Arrhenius plot of the 10-hz real surface conductivity: x, pure ice, o 10^{-4}M NaCl ice; 10^{-3}M NaCl ice.

transfer are consistent with the surface conductivity measurements.

When calculating the time constant for inductive charge flow when two ice spheres interact, Gaskell (1981) considered the constriction resistance and capacitance of two 'touching' spheres, and after several approximations, derived a value of 100usecs. This was obtained using a surface conductivity of 10^{-10}mho for pure mono-crystalline ice. A more appropriate value for the surface conductivity when the mechanism is working at 50% efficiency would appear to be 2 10^{-8}mho at 10Hz and 10^{-7}mho at 30kHz; leading (with these assumptions) to relaxation times of 0.5usec and 0.1usec respectively. We are presently measuring the contact times directly by an electrical method.

It appears that for the inductive mechanism to operate the doping of the ice should be equivalent to more than 10^{-4}M NaCℓ. Measurements of the contaminants in precipitation at the ground yield higher values than those in-cloud, and may be in error due to below cloud scavenging. Wisniewski and Cotton (1974) collected cloud water from near cloud-base inland and found NaCℓ concentration of about 5 10^{-6}M, and Takahashi (1963) from melted soft hail pellets observed values nearer 10^{-4}M, and so it seems that the 10^{-4}M NaCℓ level would be rarely reached inside active thunderstorms.

5. CONCLUSION

From this series of experiments it appears that the inductive mechanism is only significantly obeyed for ice particles having a conductivity considerably higher than that of the ice occurring naturally in the atmosphere, and we are forced to conclude that for ice-ice interactions the inductive mechanism cannot account for the observed electrification of thunderstorms. Non-inductive charging of the ice particles of the correct sign is observed at low levels of contamination, but doping the ice appears to quench this mechanism of charge transfer.

6. ACKNOWLEDGEMENTS

This work has been performed with the support of the Meteorological Office and the EOARD (grant AFOSR 82-0323). Travel funds were provided by NERC under grant GR/5384. We would like to thank Peter Kelly for his advice and help in the workshop, and Stephen Marsh for his assistance in the laboratory.

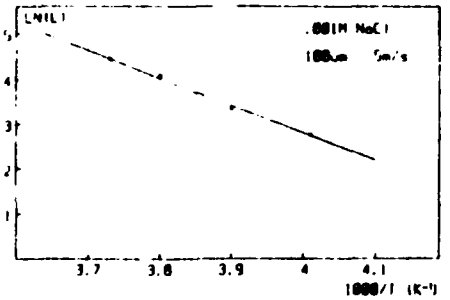

Figure 9. Arrhenius plot of the percentage of the charge leakage (L) from the 100μm particle to the target 10^{-3}M NaCℓ ice.

7. REFERENCES

Abbott,C.E., and Cannon,T.W. 1972: A droplet generator with electronic control of size, production rate, and charge. Rev.Sci.Inst.43,1313-1317.

Aufdermaur, A.N., and Johnson,D.A. 1972: Charge separation due to riming in an electric field. Quart.J.R.Met.Soc.98,369-382.

Buser,O., and Aufdermaur, A.N. 1977: Electrification by collision of ice particles on ice or metal targets. In Electrical Processes in Atmosphere, Steinkopf, Darmstadt.

Caranti,J.M., and Illingworth,A.J. 1983: Frequency dependence of the surface conductivity of ice. J.Phys.Chem.87,4078-4083.

Gaskell,W., and Illingworth,A.J. 1980: Charge transfer accompanying individual collisions between ice particle and its role in thunderstorm electrification. Quart.J.R.Met.Soc.,106,841-854.

Gaskell,W. 1981: A laboratory study of the inductive theory of thunderstorm electrification. Quart.J.R.Met.Soc.,107,955-966.

Gross,G.W. 1982: Role of relaxation and contact times in charge separation during collision of precipitation particles with ice targets. J.Geophys.Res.,87,7170-7178.

Latham,J., and Mason,B.J. 1962. Electrical charging of hail pellets in a polarising electric field. Proc.R.Soc.,A266,387-401.

Mason,B.J. 1972: The physics of a thunderstorm. Proc.R.Soc.Lond.,A327,433-466.

Reynolds,S.E., Brook, M., and Gourley,M.F. 1957: Thunderstorm charge separation. J.Met.,14,426-436.

Sartor,J.D. 1981: Induction charging of clouds. J.Atmos.Sci.,38,218-220.

Scott,W.D., and Levin,Z. 1970: The effect of potential gradient on the charge separation during interactions of snow crystals with an ice sphere. J.Atmos.Sci.,27,463-473.

Takahashi,T. 1963: Chemical composition of snow in relation to their crystal shapes. J.Met.Soc.Japan. 41,327-336.

Takahashi,T. 1978: Riming electrification as a charge generation mechanism in thunderstorms. J.Atmos.Sci.,35,1536-1548.

Wisniewski,J., and Cotton,W.R. 1974: Chemical analysis of South Florida'a environment. Proc.A.E.C. Symp., Precipitation Scavenging, Champaign.

To be presented at the Sixth International Atmospheric Electricity Conference 3-8 June 1984, SUNYA, Albany, New York, USA; then submitted to J Geophys. Res.

THE CHARGING OF ICE BY DIFFERENCES IN CONTACT POTENTIAL

J M Caranti+, A J Illingworth* and S J Marsh*

*Physics Department, UMIST
Manchester M60 1QD, ENGLAND

+IMAF, Cordoba 5000, ARGENTINA

1. INTRODUCTION

There is a widespread belief that the electrification of thunderstorms results from the charge transferred when small ice crystals collide with larger graupel or soft hail pellets. Many laboratory experiments have been carried out which have simulated these interactions (summarised by Jayaratne *et al*, (1983). Although the larger particle frequently acquired a negative charge, so that gravitational separation of the precipitation and the crystals would lead to the observed positive dipole structure of a thunderstorm, attempts to identify the precise mechanism responsible for the charge flow have not yielded conclusive results. There must be some asymmetry in the collision between the larger particle which is growing by riming and the smaller vapour grown ice crystal. Temperature gradients and resulting thermoelectric potentials do not seem to be large enough (Gaskell and Illingworth, 1980); the Workman-Reynolds freezing potentials, although of large magnitude, do not appear to develop in natural cloud conditions (Caranti and Illingworth, 1983), and the low conductivity of ice found in the atmosphere prevents the inductive mechanism from operating (Illingworth and Caranti 1984).

Buser and Aufdermaur (1977) found that when clouds of small ice crystals collided with various metal targets at -40°C the charge transfer depended upon the work function (or contact potential) of the metal. They suggested that ice formed in different ways in the atmosphere could have different contact potentials, and that this difference would cause the observed transfer when they collided. They suggested that charging could result from the difference in contact potential of evaporating ice and ice covered with frost found by Takahashi (1973). Caranti and Illingworth (1983) could not detect this difference between evaporating and condensing ice, but found that the contact potential of an ice surface changed by up to half a volt when it was rimed.

In view of the importance of the results of Buser and Aufdermaur we report further work on charging due to differences in contact potential under conditions which are more representative of those found within natural thunderclouds.

Possible unrealistic aspects of the earlier work are listed below:

a) The interactions were studied at -40°C whereas the active charging region of a thunderstorm is thought to be closer to the -10°C isotherm. At these lower temperatures the surface of the ice will have very different properties; the adhesive forces are much lower or even absent, the conductivity of the ice is much reduced, and the ice is much harder (Hobbs, 1974).

b) The small ice particles were produced by spontaneous freezing of droplets at -40°C. Such rapid freezing will tend to produce polycrystalline ice with many imperfections, which will be under great mechanical stress.

c) The frozen ice spheres were 10-40μm in size, whereas from field observations crystal sizes are often larger than this.

d) When the cloud of ice crystals impacted upon the target a current was measured, and charges per interaction derived from an estimated crystal concentration. The crystals may have received a spurious net charge from collisions with the wall of the wind tunnel, which they subsequently communicated to the target if collected.

2. APPARATUS

The apparatus for measuring individual charge transfer is shown in Figure 1 and is similar to that described in detail by Caranti and Illingworth (1984), apart from the absence of field rings and the use of removable targets made of different metals. Individual 100μm drops

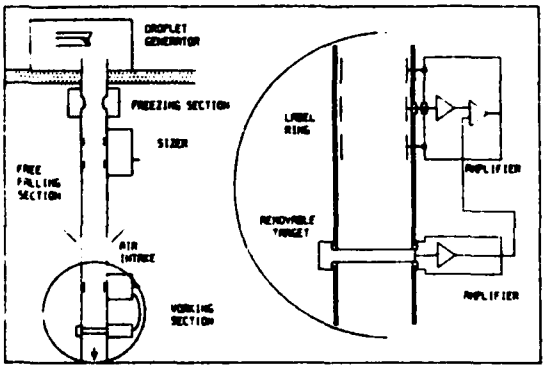

Figure 1: The apparatus for measuring individual charge transfers. Not to scale.

with controllable electric charge were produced by the drop generator on top of the cold room. They then fell in to the cold room and passed along a short section of tube where the temperature was chilled below -10°C, and a tenuous ice cloud formed, which nucleated each drop and caused it to freeze slowly. The terminal velocity, and hence the size, was measured by the time to pass between two induction rings. The ice spheres were accelerated to $10ms^{-1}$, and then passed through a final induction ring to monitor the charge before they collided with the 4mm diameter cylindrical target.

This arrangement overcomes some of the difficulties identified in the previous section. The interactions occurred at a more representative temperature, the small ice particles were frozen much more slowly, their size was slightly larger, and, most importantly, the charge transfer in each event was measured. This removed the problems of uncertain crystal concentrations, and, by monitoring the charge on each sphere before impact, any spurious charging due to collisions with the walls could be recognised and rejected. The amplifiers had a short rise time so that rapidly changing signals induced by the movement of charged ice particles could be detected. The amplifier had a long (100msec) decay time constant for any charges deposited on the target, and so actual charge transfers could be identified by the slow exponential decay which followed them.

Unfortunately, it is not possible to grow individual 100um ice crystals with a specific charge, and then accelerate them in a controlled manner to impact upon the target, so it was felt that, although the use of 100um slowly frozen water droplets does not precisely reflect conditions within the cloud, it represented a reasonable compromise.

3. RESULTS

The experiments were carried out using 100um ice particles prepared from distilled water having a conductivity of better than $2\ 10^{-6}$ mho cm^{-1}. The metal targets were either freshly plated brass (for Ag and Ni), freshly plated aluminium (for Mg), or cleaned solid rods in the case of carbon and brass. In all cases the temperature was -10°C and the impact velocity was $10ms^{-1}$.

Each small ice sphere was given an initial charge so that genuine events could be recognised by a regular train of pulses of known height from the induction ring upstream of the target. Any events not occurring with the frequency of the generator or not carrying the correct initial charge were rejected. This was most important as it enabled the spurious charge transfers due to extraneous ice crystals or specks of dust hitting the target to be excluded from the analysis.

An initial series of experiments was carried out with large (±30fC) positive and negative initial charges on the small ice particle, but there was no significant difference in the charge acquired by the target for the two polarities. It appears that with ice of such low conductivity the initial charge on the ice sphere does not have time to 'leak' to the metal target during the short time available for the interaction, and so plays no part in the charge transfer. However, in the subsequent work, the label was kept to the smallest possible magnitude (5fC), just above the amplifier noise level of 2fC.

Target	Charge Transfer (F)			Sample Size
Mg	24.6	±	15.4	87
Mg	29.7	±	21.6	123
Zn	-16.9	±	21.4	120
Zn	-17.3	±	25.0	252
C	-20.3	±	11.6	85
Brass	-21.3	±	13.1	186
Ag	-62.4	±	30.8	255
Ni	-70.3	±	49.1	266

Table 1: Average charge transferred to different targets.

Table 1 summaries the charge transfers measured for the various targets. Although the standard deviations initially appear to be large, the anomalous positive charging of the magnesium target immediately stands out. Figure 2 displays histograms of each charge transfer for the first three runs in Table 1, and it can be seen that although the mean is well defined there is a considerable spread of the individual results. For magnesium all the transfers are positive, but in the case of zinc, although the mean is negative, occasional positive transfers are observed.

The histograms for the charge transfers for the other metallic targets are shown in Figure 3. For these metals each individual transfer is negative. All the histograms have the same general shape, and in each example a skew distribution about the mean is in evidence. The maximum transfers are over twice the mean, for example, nickel has a mean of -70, but some transfers exceed -140fC. This suggests that there is some randomness in the transfer process itself, and that the standard deviations in Table 1 should not be interpreted as errors. From an examination of the histograms it is evident that the expectation values for the charge transfer to the different targets are significantly different.

Although the work functions of the individual metals were not monitored in this experiment, values taken from the Handbook of Physics and Chemistry are plotted in Figure 4 against the average charge transfers from Table 1. A general correlation is evident, confirming the results of Buser and Aufdermaur.

If the ice collided with a metal and no charge transfer occurred, we would deduce that they had the same contact potential or 'work function'. From this definition, the data in Figure 4 imply a 'work function' of the ice of 4.2eV. To investigate this further a series of experiments was performed to measure the contact potential of ice against various metals. The Kelvin capacitor method, as described by Caranti and Illingworth (1983), was employed. The upper electrode was always gold plated, and the lower electrode consisted of the same ice sample which was placed in turn on various metals (Pt, Pd, Ag, Hg, Cu, Sn, Al, Mg). If the ice was acting as a perfect insulator, then the apparatus would detect the change in work function of the lower metal electrode, but if the ice acts as a conductor, the arrangement acts as a gold-ice capacitor with constant contact potential irrespective of the metal under the ice. In fact the results were intermediate and a plot of measured contact

potential against work function of the lower metal had a gradient, not of unity or zero, but of 0.5. This plot also predicts that ice should have zero contact potential against a metal with a work function of 4.3eV.

Some preliminary collision experiments have been carried out using an ice covered target. We hope to report on these more fully when the analysis is complete. Figure 5 shows a histogram of the charge transfers at -10°C, and we draw attention to the same general skew distribution of the individual charge transfers that is evident for ice-metal collisions in Figures 2 and 3.

4. CONCLUSION

The charge transferred when small 100μm diameter ice spheres collide with various metal targets shows a clear dependence upon the work function of the metal. The situation for ice-ice collisions inside natural clouds is different, because a metal contains free electrons but the lifetime of an electron inside ice is less than 0.1nsecs (Kunst and Warman, 1980). Measurements of the photo-electric effect (Nason and Fletcher, 1975) give a value of 6.3eV for the work function of electrons in ice, but the indirect methods reported here suggest the apparent value for the charge carriers is nearer 4.3eV. In view of the finding that the initial charge on the small ice crystal does not affect the transfer, we must assume that the charges flowing in ice-ice or ice-metal collisions are not electrons and are actually resident on the ice surface at the point of impact. These carriers may be the free ions in the amorphous non-crystalline layer on the ice surface (Fletcher, 1968). Since such layers would exist on both surfaces during an ice-ice collision, a difference in contact potential of the two ice surfaces should cause a charge to be transferred.

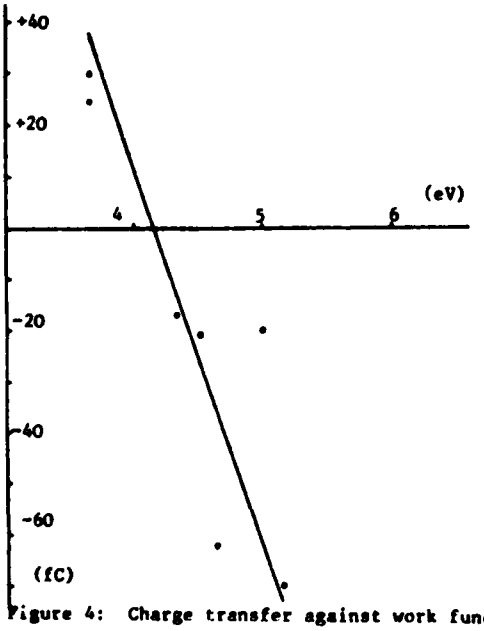

Figure 4: Charge transfer against work function

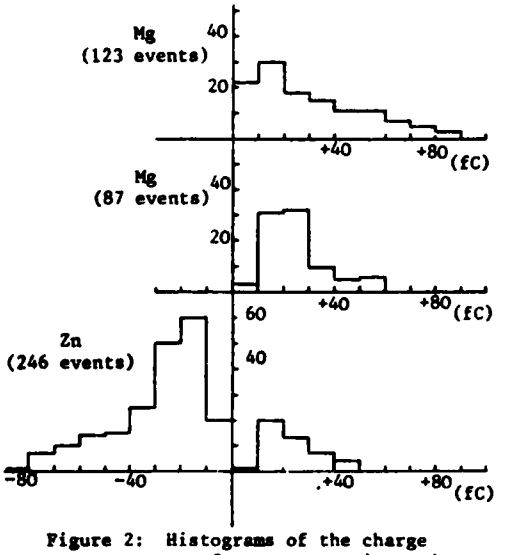

Figure 2: Histograms of the charge transfers to magnesium and zinc targets.

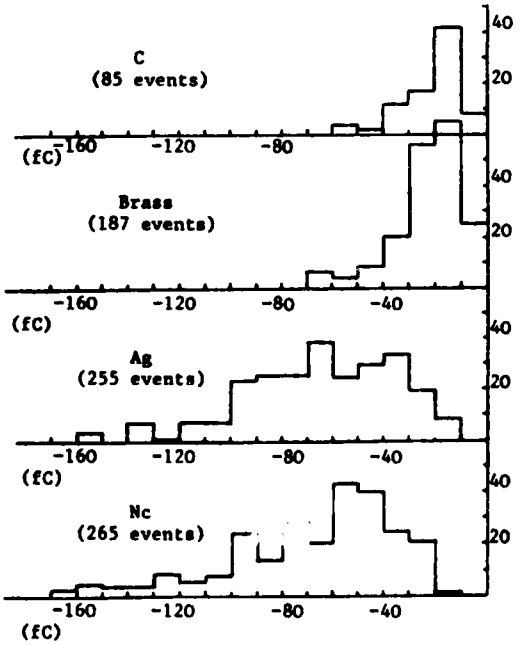

Figure 3: Histograms of the charge transfers to carbon, brass, silver and nickel targets.

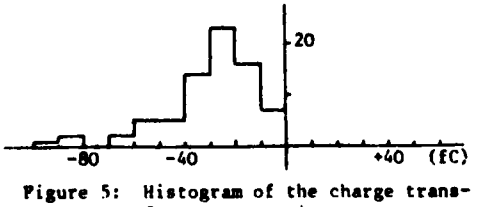

Figure 5: Histogram of the charge transfer to a pure ice target at -10°C.

5. ACKNOWLEDGEMENTS

This work has been performed with the support of the Meteorological Office and the EOARD (grant AFOSR 82-0323). Travel funds were provided by NERC under grant GR/5384. We would like to thank Peter Kelly for his advice and help in the workshop.

6. REFERENCES

Buser,O., and Aufdermaur, A.N. 1977: Electrification by collision of ice particles on ice or metal targets. In Electrical Processes in Atmosphere, Steinkopf, Darmstadt.

Caranti,J.M. and Illingworth,A.J. 1983: The contact potential of rimed ice. J.Phys.Chem.,87. 4125-4130.

Caranti,J.M. and Illingworth,A.J. 1983: Transient Workman-Reynolds freezing potentials. J.Geophys. Res.,88,8483-8489.

Fletcher,N.H. 1968: Surface structure of water and ice. II. A revised model. Phil.Mag.18,1287-1300.

Gaskell,W., and Illingworth,A.J. 1980: Charge transfer accompanying individual collisions between ice particle and its role in thunderstorm electrification. Quart.J.R.Met.Soc.,106,841-854.

Hobbs,P.V. 1974: Ice Physics. Clarendon Press, Oxford.

Illingworth,A.J. and Caranti,J.M. 1984: Ice conductivity restraints on the inductive theory of thunderstorm electrification. (These proceedings).

Jayaratne,E.R., Saunders,C.P.R. and Hallett,J. 1983: Laboratory studies of the charging of soft-hail during ice crystal interactions. Quart.J.R. Met.Soc.,109,609-630.

Kunst,M. and Warman,J.M. 1980: Proton mobility in ice. Nature,288,465.

Nason,D. and Fletcher,N.H. 1975: Photoemission from ice and water surfaces. Quasiliquid like layer effect. J.Chem.Phys.,62,4444.

Takahashi,T. 1973: Electrification of growing ice crystals. J.Atmos.Sci.,30,1220-4.

To be presented at the International Aerospace and Ground Conference on Lightning and Static Electricity, 26-28 June 1984, Orlando, Florida, USA.

STATIC CHARGING OF DIFFERENT METALS BY ICE CRYSTALS

+J. M. Caranti, *A. J. Illingworth and *S. J.Marsh
*Physics Department, UMIST, Manchesterr M60 1QD, England
+IMAF, Cordoba, 5000, Argentina

ABSTRACT

It is known that aircraft usually charge negatively when they fly through clouds. We report laboratory experiments which show that for speeds of up to 80ms^{-1} small ice particles charge most metal targets negatively, but that magnesium acquires a positive charge. The charge transfer was found to be proportional to the impact velocity and to the square of the size of the ice particle. It appears that the charging is controlled by the work function of the metal.

INTRODUCTION

AIRCRAFT GENERALLY ACQUIRE negative charge when they fly through clouds, as a result of the triboelectric or frictional charging occurring when water or ice particles in the cloud collide with the aircraft surface. Effort in the past has been directed towards characterising the currents expected in different meteorological conditions, and then designing an efficient method of discharging the aircraft. However, modern aircraft constructed from composite materials may have different charging properties from conventional ones, and, furthermore, any interference in modern digital control systems is potentially more hazardous than for the traditional analogue methods.

Tanner (1) has reported current densities for aircraft to be in the range 50-100 $\mu A.m^{-2}$ for cirrus clouds, 100-200 $\mu A\ m^{-2}$ for stratocumulus, and 300 $\mu A\ m^{-2}$ for snow. Boulay and Laroche (2) measured the current to probes covered with conducting paint on a Meteor aircraft flying at 200 ms^{-1}, and confirmed these values. They estimated that the overall capturing area of the aircraft was about $8m^{-2}$, and calculated the maximum charging current to be 3mA, which compared well with the highest discharger current recorded of over 2mA. On only one occasion, in liquid precipitation near the ground, did they record positive current. In an investigation which extended to higher speeds, Nanevicz (3) also measured current in the range 100-200 $\mu A\ m^{-2}$, but, in addition, observed the ice crystal concentration. At mach 1.2 he estimated that each ice crystal collision transferred about 50pC, the value was slightly higher at 200ms^{-1}, but at mach 1.9 the charge per interaction was reduced by about 50%.

At an earlier conference (4) we suggested that the charging occurring when ice crystals collided with metals depended upon the work function (or contact potential) of the metal and the ice. In that laboratory study the velocities of up to 10ms^{-1} were unrealistically low, and it is not clear that the same charging mechanism should operate at higher velocities when cracking and fracturing of the ice may occur (5).

We now report the results of an experiment in which ice particles of size from 50 to 100μm were accelerated to speeds between 10 and 80 ms^{-1} and the charge transfer measured when they collided with various metal targets. This particle size range is appropriate for crystals occurring naturally in clouds which are responsible for most precipitation static. Trinks and ter Haseborg (5) have carried out experiments with 20mm diameter ice projectiles to simulate the effect of hailstone charging. Such large particles were totally pulverised when they hit metal targets at speeds in the range 35 to 1000 ms^{-1}. The targets acquired negative charges of up to 10pC per interaction, but the total number of these violent collisions in a cloud should be low.

APPARATUS

Water droplets in the size range 50-200μm with a controllable charge (0 to ±250fC) were produced at the rate of about 1Hz by an Abbott and Cannon (6) droplet generator on top of the cold room. Each droplet then froze slowly as it fell down a tube into the cold room and collided with a tenuous cloud of minute ice crystals, which was formed by cooling a short section of the tube. The time for the particle to pass between two induction rings placed just below the freezing section then enabled the terminal velocity of each particle to be determined, and hence the size estimated to better than 10μm. After falling a further 45cm, sufficient for the 100μm particles to freeze completely and reach thermal equilibrium, the particles were accelerated to speeds of up to 80ms^{-1} by compressed air. The compressed air was introduced at the periphery of the tube between two co-axial cones with an adjustable separation of about 1mm. This symmetric conic jet served to centre and to accelerate the small ice particles. The accelerated ice particles then passed through a final induction ring before hitting the target. The target was a cylinder 4mm in diameter and was easily removable so that the charging properties of different materials could be investigated.

Separate amplifiers were placed as close as possible to both the induction rings and the target to reduce microphonic and 50Hz pick up to the equivalent of less than 2fC. The amplifier outputs were summed, recorded, and subsequently replayed and examined on a digital storage oscilloscope. Because the amplifier has a rise time of 3μsecs but a long (100msec) decay time for any charge deposited on the target, it was possible to differentiate between the rapidly varying induced charges caused by approaching and departing charged particles, and the long 100msec exponential decay when charge was transferred to the target. Considerable information on the nature of the interaction could be derived from the shapes of the waveforms as shown in Figure 2.

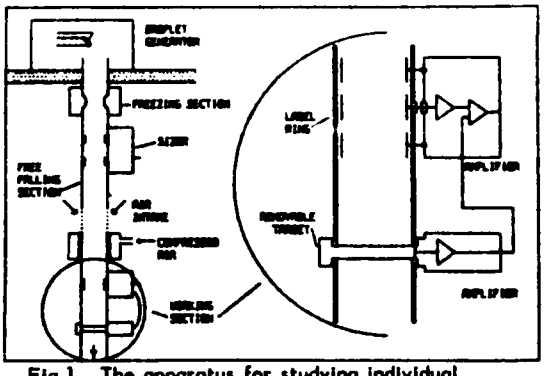

Fig.1. The apparatus for studying individual collisions of ice particles with various metal targets.

In all cases the first pulse is the passage of the particle through the induction ring with its initial label charge, q_i. The start of the second excursion of each waveform is the charge induced on the target as the particle approaches, and from the elapsed time since the passage through the induction ring the velocity of impact may be calculated. Subsequently, on actual collision a variety of waveforms are possible transferring charge q_t to the target as shown in Figure 2 and described below:

a) If the second pulse is smaller than the first, then the particle has just missed the target, such waveforms are of great help when trying to align the apparatus. When the two pulses are equal there is ambiguity; either the particle has passed very close to the target but just missed it, or it has collided and separated but no charge has been transferred,
b) Either the particle has hit the target and stuck to it - a 'collection'; or it has collided, donated its charge to the target, and then left carrying no charge
c) The particle has collided with and separated from the target, transferring to the target an amount of charge (q_t) equal to a fraction of the initial charge (q_i) on the particle.

d) Positive charge (>q_i) has been acquired by the target.
e) Negative charge has been acquired by the target.
f) as for d), but after collision the ice particle has rebounded upstream and then been accelerated and passed close to the target within 'electrostatic range' inducing the blip superposed on the exponential decay.
g) An extreme case of f) in which the particle has rebounded upstream and then bounced a second time on the ice target and transferred additional charge during the second interaction.
h) Initially appears to be similar to a), but the presence of the third pulse confirms that the particle has bounced upstream and then passed close to the target; this cannot be a collection but must indicate an interaction with zero charge transfer.

In examples f), g) and h) the rebounding and subsequent sensing of the particle indicate a more head-on collision, whereas the earlier waveforms will tend to reflect a more equatorial or grazing interaction. There is an equivalent set of waveforms for negative initial label charge. On occasion more complex waveforms are observed which initially appear to violate charge conservation, until it is realised that the particle must have bounced from the target to the wall where it acquired a spurious charge being sensed by the target amplifier a second time. Such pulses were rejected.

RESULTS

The experiments were carried out with ice particles made from distilled water having a conductivity of less than 1.5 10^{-6} mho cm^{-1}, which is appropriate for natural ice occurring in the atmosphere. In all these studies the temperature was kept at -10°C. Most materials were found to charge negatively, but one important exception was magnesium which charged positively over the range of velocities covered in this study. Figure 3a shows an event in which a 100μm ice particle transferred + 1200fC to a magnesium target. From the 1.5msec delay between the sensing of the initial charge (q_i) of 160fC and the time to hit the target 12cm below, an impact speed of 80ms^{-1} was derived. The interaction in Figure 3b is similar with the magnesium target receiving +880fC, but in this case the waveform is of the type shown in Figure 2f, suggesting that the small ice particle has bounced upstream and then been reaccelerated and passed close to the target. At these high speeds

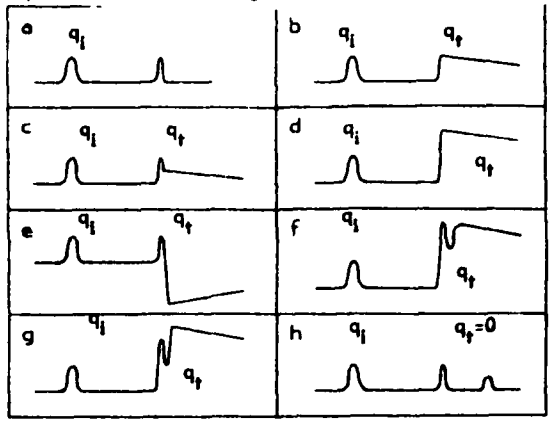

Fig.2. - A selection of the various possible waveforms from the amplifiers. For explanation see the test.

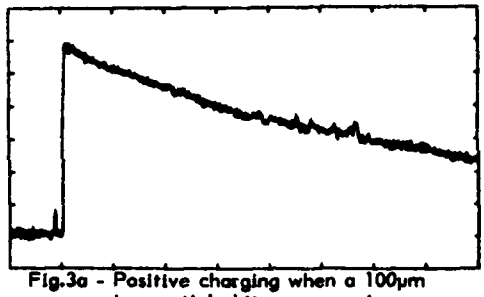

Fig.3a - Positive charging when a 100μm ice particle hits a magnesium target at 80ms^{-1}. Horiz scale 10msec per division, vert scale 200 fC per division -10°C.

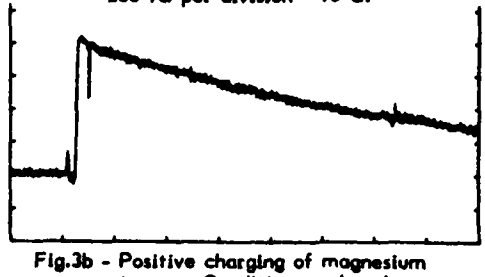

Fig.3b - Positive charging of magnesium target. Conditions and scales as for 3a.

P3
CAMPBELL, ICE, & MARSH

the microphonic noise is equivalent to 30fC. Figure 4a displays the charging of a nickel target by -250fC when hit by a 100μm ice particle at $10ms^{-1}$, and again in this example the particle bounces and subsequently passes near to the target. Typical charging of a brass target covered with polyurethane paint is shown in Figure 4b, in this case the target receives a charge of -400fC from a $60ms^{-1}$ interaction, with microphonic noise now reduced to 15fC. On this expanded time scale the shape of the induced pulse as the particle approaches and leaves the target is clearly visible, and from these slopes it is possible to derive the velocities of approach and separation and to examine the mechanics of the collision in more detail.

In both Figure 3 and 4 the initial charge (q_i) is a small fraction of the total charge transferred (q_t) to the target. A series of preliminary experiments with much larger initial charges confirmed that q_i was not affecting the charge transferred to the target, and that q_i could be regarded as an identifier 'label'. It appears that in the short time available, the initial charge carried by the small ice particle is not able to migrate along the surface of the ice to the area of contact of the ice and metal, where it could affect the charge transfer. This is in accordance with our knowledge of the surface conductivity of ice (7); however, to minimise any possibility of interference the initial charge was kept to the smallest value which still allowed the particle to be identified as it passed through the induction ring, and permit definite confirmation of genuine events. Any charge transfers which were not preceded by the correct label at the correct time before contact with the target were probably due to spurious dust particles or extraneous ice particles, and were excluded from the analysis. In this way unambiguous waveforms as displayed in Figures 3 and 4 predominated, and problematic waveforms of the type shown in Figure 2 a,b,c, and h with their attendant difficulties of interpretation were avoided.

When histograms of the charge transfers for many events under a given set of conditions were plotted, they showed the same general features found for low speed ice-metal collisions reported previously (8); the distribution was skew with a tail of large transfers having magnitudes twice or three times the mean. The shapes of these histograms suggest that there is some random process in the charge transfer process itself, and that although the calculated standard deviations for the charge transfer was usually about half the mean value, the expectation value for the transfer was fairly well defined when 40 events were taken together.

Figure 5 shows a plot of the average charge transfer for ice impacting upon magnesium and nickel targets as a function of velocity. Before each run both targets were freshly polished. There was some evidence of changes in magnitude of up to 50% as the magnesium target aged, but this ageing did not affect the sign of the transfers. The trend from the Figure is quite clear, with an approximately linear increase with velocity for the positive charging of

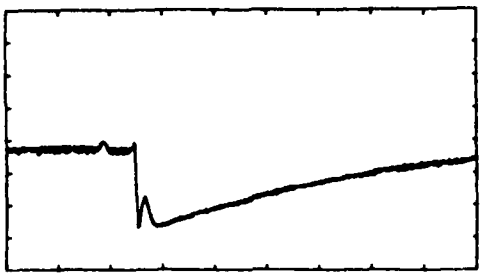

Fig.4a - Negative charging of a nickel target at $10ms^{-1}$ by a 100μm ice particle, at -10°C. Horiz scale 20msec per division, vert 100fC per division.

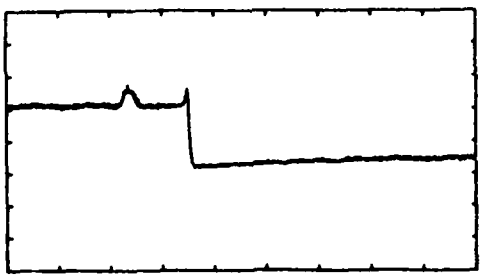

Fig.4b - Negative charging of brass covered with polyurethane paint. $60ms^{-1}$. Horiz scale 2msec per division, vert scale 200fC per division.

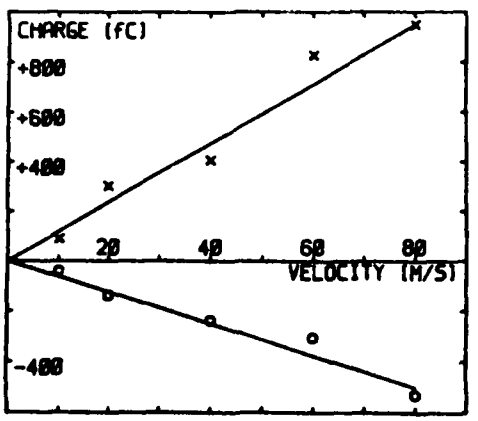

Fig.5 - The charge transferred to magnesium (X) and nickel (O) targets as a function of velocity by 100μm ice particles at -10°C.

the magnesium and for the negative charging of the nickel. With the compressed air available it was difficult to attain velocities of 100ms^{-1}, but from a limited amount of data the increase in charge with velocity appeared to extend to thishigher speed.

In order to examine the effect of size on the charge transfer a series of experiments was performed using ice particles in the size range 75 to 220 μm and a nickel target. For some of the interactions with the largest particles positive charging was found, and these events were often accompanied by complex waveforms of which Figure 6 is a typical example. From this Figure it seems that there is bouncing and break up into three fragments which subseuqently pass close to the target; one or more of the fragments may have received additional charge from a rebound off the walls of the tube. It appears that although the 45cm long free fall section of tube is long enough for complete freezing of the 100μm particles, because of the mass increase and greater terminal velocity, the 200μm particles are only partially frozen and so are likely to disintegrate when hitting the target.

Figure 7 displays the average charge transfer as a function of the square of the size of the ice particles for collision velocities of 10 and 60ms^{-1}. Data for sizes above 200μm have not been included because of the fragmentation problems discussed above. For the 10ms^{-1} run with 183μm particles about one third of the events resulted in positive charge transfer with an average value of +198fC, but only the two thirds which gave simple waveforms with negative charging have been included in the analysis. No positive events were observed for the other points shown on the graph. For the experiments at 60ms^{-1} the compressed air was interfering with the droplet generator and so some difficulty was experienced in keeping the droplet size constant and is responsible for the increased scatter. For both velocities, it is clear that the average charge transfer is increasing with velocity, and there is strong evidence for a square law dependence. A short experiment using 130μm supercooled liquid droplets at 60ms^{-1} with a nickel target confirmed positive charging for non-frozen particles with an average transfer of +120fC.

Experiments (8) at 10ms^{-1} have shown a good correlation of charge transfer with the work function of the metal, but we have not yet completed a comprehensive study at the high speeds. However, target of barium oxide, which has a low work function charged consistently positively at high speeds. Other materials including aluminium, carbon and silver charged negatively. When 100μm particles at 60ms^{-1} and a target of brass covered with polyurethane paint were used, an average transfer of -670fC was measured, a teflon covered target resulted in an average value of -500fC, and a target covered with smooth ice also charged negatively but to a lesser degree.

The ice crystals occurring in the atmosphere are vapour grown and have different shape and momentum from the spherical particles used in this experiment. At the start of each experiment a cloud of minute ice crystals would form in the cooled section of the free fall tube, and this cloud would persist for a few minutes, and give rise to occasional clearly observable charging events when the crystals hit the target. Such events were not preceded by a recognisable label and so, because of the unknown size of the ice crystal, were not included in the analysis, however, the crystals always gave the same sign of charging as the controlled ice spheres. The low work function magnesium charged positively and the nickel acquired negative charge.

CONCLUSION

The charging of metal targets by small ice particles increases linearly with velocity for speeds of up to at least 80ms^{-1}, and is approximately proportional to the square of the particle size for spheres of diameter up to 200μm. Gaskell and Illingworth (9) found a similar dependence for ice-ice collisions at much lower speeds of less than 12ms^{-1}, and observed that these results implied that the charge transfer was proportional to the contact area (A) predicted by elastic collision theory to vary as

$$A \propto v^{4/5} r^2 \qquad (1)$$

where v is the velocity and r the radius of the small particle. Work on collisions below 10ms^{-1} (8) has shown that the charge transfer depends upon the work function of the metal, and if the work function (or contact potential) difference between the metal and the ice is V, then the charge transfer should be given by

$$q = CV \qquad (2)$$

where C is the capacitance as the small particle separates from the target and is proportional to the contact area A in equation 1. The positive charging observed at the higher speeds in this paper by magnesium and barium oxide targets, and the negative charging for other targets with larger work functions indicate that the differences in contact potential are controlling the charge transfer at these higher speeds.

Partially frozen and liquid drops appear to charge targets positively; positive charging by splashing water drops at much lower speeds has been explained in terms of the disruption of the electric double layer (10).

The negative charging found in this study with most common metals and paint covered targets is consistent with the negative charging observed with aircraft. Direct quantitative comparison of the laboratory studies with aircraft measurement involves an assumption of the typical size and concentration of ice particles in clouds. The charge per interaction for a 100μm particle has been found to be about -1pC at 80ms^{-1}. From our derived velocity and size dependence this would suggest that a 200μm particle at 200ms^{-1} would charge a target by about -10pC. If the concentration was 100 per liter then the current would be about 200μa m^{-2}, in agreement with most densities reviewed in the introduction. Boulay and Laroche (2) recorded one occasion of positive charging in rain, which is compatible with our findings with liquid drops. Nanevicz (3) found a charge per crystal of about -50pC at much higher velocities. It would be of interest to fly magnesium probes to see if they charged positively.

We plan to continue this work extending the interactions to higher speeds, and also to investigate the properties of other materials. At present some targets charge positively and others negatively, alloys may exist which give zero charging. Such materials would appear to minimise any static charging to aircraft.

ACKNOWLEDGEMENT

This work has been performed with the support of the Meteorological Office and the EOARD (grant AFOSR 82-0323). Travel funds were provided by NERC under grant GR/5384. We would like to thank Peter Kelly for his advice and help in the workshop.

REFERENCES

1. R.L. Tanner, et al., "Precipitation Charging and Corona-Generated Interference in Aircraft", Technical Report No. 73, Project No. 2494, Contract AF 19 (604) 3468, 1961.

2. J.L. Boulay and P. Laroche, "Aircraft Potential Variations in Flight", Eighth Lightning and Static Electrification Conference, Forth-Worth , 1983

3. J.E. Nanevicz, "Flight-Test Studies of Static Electrification on a Supersonic Aircraft", Lightning and Static Electrification Conference, Culham, 1975.

4. J.M. Caranti, and A.J. Illingworth, "Static Charging by Collisions with Ice Particles", Lightning and Static Electrification Conference, Oxford, 1982.

5. H. Trinks, and J.L. ter Haseborg, "Electric Charging by Impact of Hailstones and Raindrops", Eighth Lightning and Static Electrification Conference, Forth Worth, 1983.

6. C.E. Abbott, and T.W. Cannon, "A Droplet Generator with Electronic Control of Size, Production Rate, and Charge", Rev. Sci. Inst. 43, 1313-7, 1972.

7. A.J. Illingworth and J.M. Caranti, "Ice Conductivity Restraints on the Inductive Theory of Thunderstorm Electrification", VIIth Int. Conf. on Atmos. Electricity, Albany, New York, 1984.

8. J.M. Caranti, A.J. Illingworth, and S.J. Marsh, "The Charging of Ice by Differences in Contact Potential", VIIth Int. Conf. on Atmos. Electricity, Albany, New York, 1984.

9. W. Gaskell, and A.J. Illingworth, "Charge Transfer Accompanying Individual Collisions Between Ice Particles and Its Role in Thunderstorm Electrification", Quart. J.R. Met. Soc., 106, 841-854, 1980.

10. Z. Levin and P.V. Hobbs, "Splashing of Water Drops on Solid and Wetted Surfaces", Phil. Trans. Roy Soc. A, 269, 555-585, 1971.

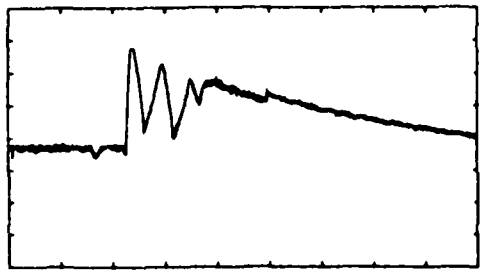

Fig.6 - Positive charging of a nickel target at 10ms^{-1} by a 183μm diameter particle. Vertical scale 100fC per division, horiz scale 20 msec per division.

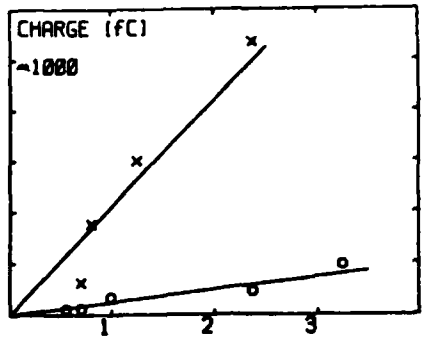

Fig.7. - The charge acquired by a nickel target as a function of the size of the ice particle X 60ms^{-1}. O 10ms^{-1}. The units of the horizontal scale are 10^{-4} μm^{2}.